INVESTIGATING THE CORRELATION BETWEEN QUALITY FACTOR OF METALLIC CAVITIES AND ELECTROMAGNETIC RADIATION

By

COREY VHLIDAL

Bachelor of Science in Electrical Engineering

Oklahoma State University

Stillwater, OK

2012

Submitted to the Faculty of the
Graduate College of the
Oklahoma State University
in partial fulfillment of
the requirements for
the Degree of
MASTER OF SCIENCE
July, 2015

INVESTIGATING THE CORRELATION BETWEEN QUALITY FACTOR OF METALLIC CAVITIES AND ELECTROMAGNETIC RADIATION

Thesis Approved:

Dr. Charles Bunting

Thesis Adviser

Dr. George Scheets

Dr. James West

Name: Corey Vyhlidal

Date of Degree: JULY, 2015

Title of Study: INVESTIGATING THE CORRELATION BETWEEN QUALITY FACTOR OF METALLIC CAVITIES AND ELECTROMAGNETIC RADIATION

Major Field: ELECTRICAL ENGINEERING

Abstract: This research investigates the correlation in reduction of quality factor of a reverberant cavity and that cavity's ability to radiate. A reverberant cavity was chosen because it provides an idealized model of many commercial electronic devices since they are usually housed in metal casings. Phase 1 of this research investigates multiple methods for optimizing the reduction in *Q* through the use of RF absorbing material. Phase 2 of this research develops an experimental approach to obtaining the electromagnetic emissions from a metallic cavity using a nested reverberation chamber approach.

This research uses a time domain method for determining the *Q* factor of a small metallic cavity. This research has shown that increasing the surface area of an absorber has a much more significant impact on reducing the *Q* of a cavity than increasing the volume of the absorbers. This research has also shown that it is more efficient to use several smaller absorbers spaced apart rather than larger single pieces. Another finding from this research is that the same *Q* levels can be reached with less material by utilizing absorber designs that increase surface area while reducing volume. This research also addresses an erroneous assumption of the time domain *Q* factor measurements that states that pulse width must be shorter than the wall scattering time in order to not adversely affect the measurements. It has been found that this requirement is unnecessary. By measuring the change in *Q* of a cavity and the change in emissions from a cavity, a correlation has been found showing that *Q* reductions from loading directly result in emission reductions, but the amount of reduction of emissions per reduction in *Q* is frequency dependent. This could mean that the results may vary from one test cavity to the next.

TABLE OF CONTENTS

LIST OF TABLES

Table Page

LIST OF FIGURES

Figure Page

Figure Page

CHAPTER I

Introduction

Every day, new electronic devices are manufactured and put into use. These devices have more features and functions than ever before. As a result of all of these new features and functions, the electronic hardware inside these devices is becoming more and more complex. In order for these devices to be used, there are restrictions on the amount of electromagnetic interference (EMI) that they can radiate. These limits are imposed by governing bodies, such as the Federal Communications Commission (FCC) or the International Electrotechnical Commission (IEC) through the adoption of emissions standards. There are different methods for combating this adverse effect. One method is to house the devices in metal cases to create an EM shield. Unfortunately, these metal cases cannot be completely enclosed cases that would provide a Faraday cage shielding. They usually require openings for wiring harnesses, airflow, or structural purposes. Many devices have communications requirements, such as tablets, phones, computers, and there has to be a way for desired waves to radiate, but unintentional radiation is unavoidable. Another method to suppress unintentional emissions is to utilize radio frequency (RF) absorbing materials that suppress the electromagnetic (EM) fields inside the enclosure to reduce the energy available to radiate. Although these absorbers are commonly used, there has only been limited research regarding their optimal usage. Design engineers need a way to be able to quantify the amount of material required so that they only use as much as needed. This research aims to

provide a step in the direction of knowledgeable usage of RF absorbers. The typical approach for using RF absorbers when failing an emissions test is to open the device, add some RF absorbing material, close the device, and retest. This process is repeated until the device passes the emissions test. While this technically achieves the desired goal of reducing emissions, there is little to no thought about using them efficiently which could save time, weight, and money.

This research seeks to find a correlation between the change in the quality factor, Q, of a reverberant cavity and the change in the amount of power radiated out of the cavity. The assumption up to this point has been that reducing the Q of a cavity through loading removes available energy from the cavity. With less energy available, less energy will radiate out. While this assumption is intuitive, it has not been verified. It has also not been verified that the reduction in Q will produce the same reduction in radiation at different frequencies. For the purpose of finding a correlation between Q and radiation, the first challenge of this research is determining an effective method for measuring the Q of a cavity. The second task of this research is to investigate how different absorber configurations affect Q. The third phase is to establish a method for measuring the power radiated from a metallic cavity. Lastly, the final goal of this research is to determine how well the Q and radiation are correlated.

This thesis is divided into 5 chapters. The next chapter provides an overview of existing work related to this research in order to provide the necessary background information to understand the context as well as need for this research. The third chapter outlines the experimental techniques used to collect the data for this research. The fourth chapter explains the results of the experiments as well as conveys the story of the evolution of this research. Chapter 4 covers the results of multiple experiments involving different strategies for reducing Q as well as the results from the radiation measurements. Chapter 4 also discusses the correlation results between the Q of a cavity and how well it radiates. Chapter 5 provides a review of the key points from each

chapter as well as the important conclusions from the results. Chapter 5 will also include avenues of future work that this research has uncovered but not sufficiently addressed.

CHAPTER II

Review of Literature

This chapter serves as a platform to provide the background information to provide the proper context in which this research can be used. Section 1 will discuss general methods for reducing emissions. It provides the background information needed for understanding the need for the use of RF absorbing material as well as some existing work in optimizing their effectiveness. Section 2 provides an overview of reverberation chambers. This will include their design, essential properties, and typical usage. Section 3 will discuss quality factor (Q) measurements for a reverberant environment for both the frequency and time domains. Section 4 will cover radiation measurement techniques.

2.1 Emissions Reduction

There is not a realistic method for creating a perfect EM shield. Enclosing a device in a metal casing is a good starting point, but there will always be various apertures that are unavoidable. Since unintentional emissions will almost always be unavoidable, the only viable approach is to reduce the emissions in the frequency regime of maximum impact. One of the major contributing factors to how well a metallic cavity will radiate is based on the size of the apertures. In [1], different aperture sizes and arrays were simulated to determine the shielding effectiveness of changing aperture sizes. In order to determine the shielding effectiveness, a Thevenin equivalent model is created to find the equivalent source voltage and impedance of the apertures. By finding

the Thevenin equivalent model, the power transferred out of the cavity can be calculated in relation to the power transferred without the metal enclosure. This ratio of the power transferred with the aperture to the power transferred without the case is the shielding effectiveness. A 30 cm × 12 cm × 30 cm cavity was simulated with a single 3 cm × 3 cm aperture, a 3×3 array of 1 cm × 1 cm apertures, and a 5×5 array of 0.6 cm × 0.6 cm apertures. In all three cases, the total aperture area remains the same, but the size of the individual apertures is decreased. Figure 2-1 shows a graph of the simulated values for the shielding effectiveness of the different apertures.

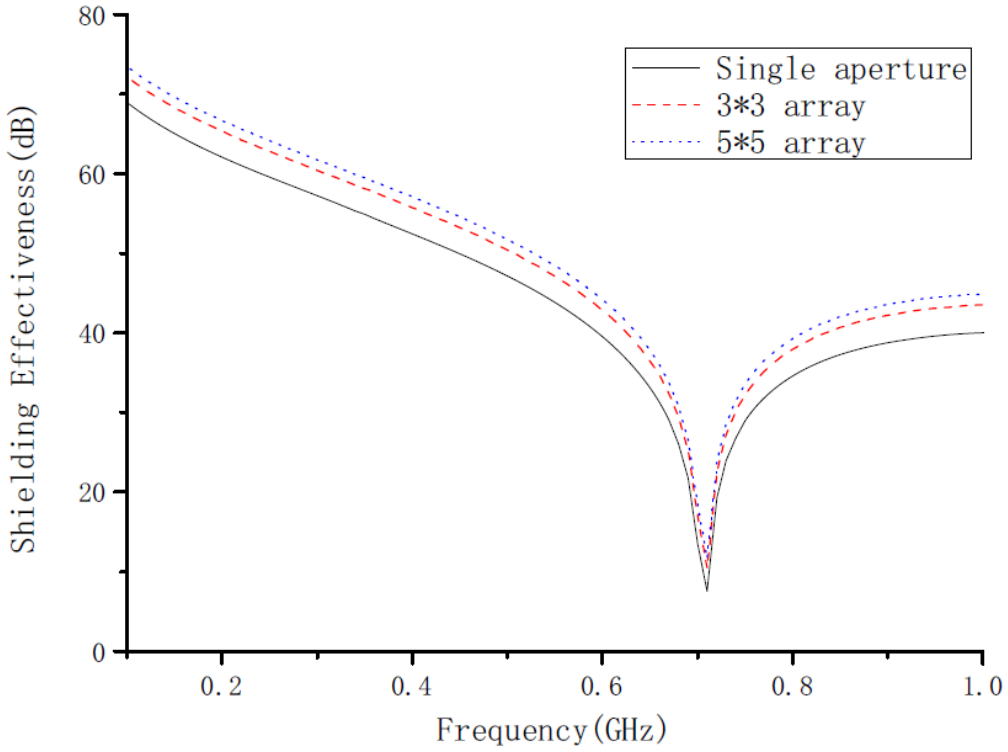

Figure 2-1: Aperture Size Shielding Effectiveness Results [1]

This figure shows that a larger number of smaller apertures results in a higher shielding effectiveness. This increase is shown by the approximately 3 dB increase in shielding effectiveness for all frequencies outside of the resonance just above 700 MHz for the 3 × 3 array over the single aperture and the approximately 1 dB increase in shielding effectiveness over all frequencies outside of the resonant frequency for the 5 × 5 array over the 3 × 3 array. This

increase in shielding effectiveness is due to the inverse relationship between aperture size and the aperture resonance frequencies. In [2], the aperture resonances are defined as the frequencies where a dimension of the aperture size is an integer multiple of λ/2. For the 3 cm, 1 cm, and 0.6 cm apertures, the lowest resonant frequencies were 5 GHz, 15 GHz, and 25 GHz respectively. Since these frequencies are much greater than the simulated frequencies, the shielding effectiveness of these apertures is very high. Unfortunately, sometimes a device will radiate over a broad range of frequencies and aperture resonances are unavoidable. Some devices may require apertures with a specific minimum size to allow for heat exhaust, airflow, or weight reduction. When aperture resizing is not an option, RF absorbers can be used to suppress emissions. In [2], Green discusses some key aspects of using RF absorbers to reduce emissions. Green used a nested cavity approach by placing the small cavity inside the ETS-Lindgren SMART 80 chamber. Figure 2-1 shows an illustration of Green's test setup.

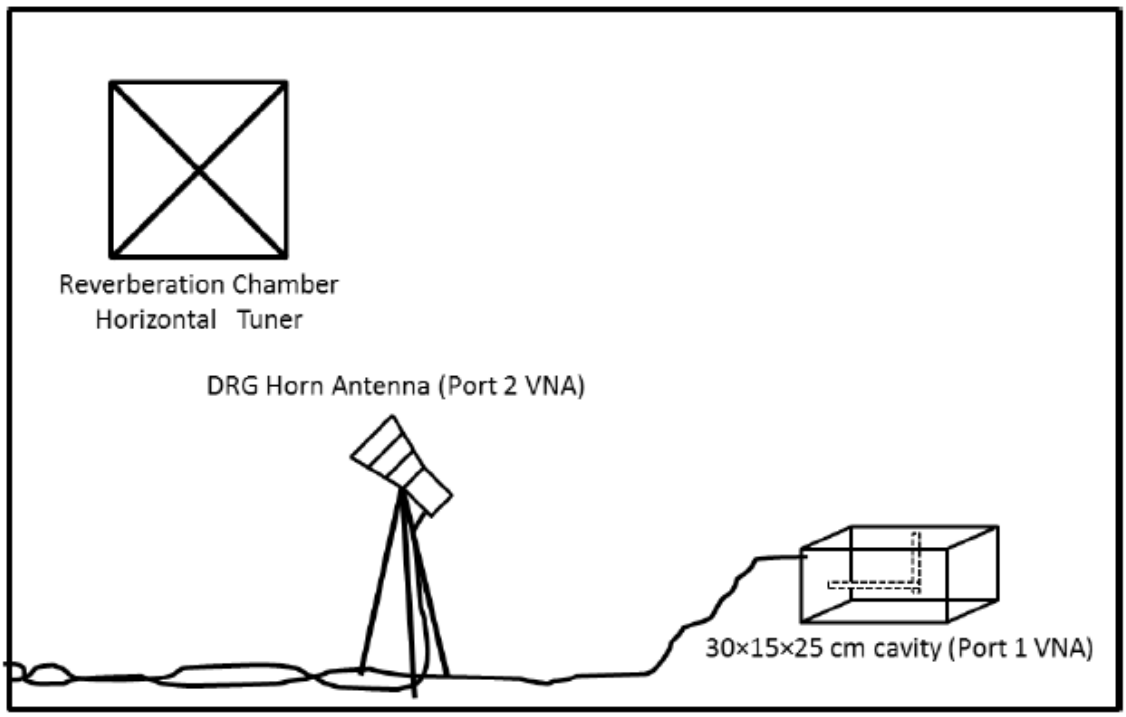

Figure 2-2: Green Test Setup Illustration[2]

A small tuner is continuously stirring inside the small cavity, and S_{21} is measured for 50 independent tuner positions for the SMART 80 tuner. Green defines absorber effectiveness, *A.E*, as:

$$A.E. = < S_{21} >_{No\ Absorber} - < S_{21} >_{Absorber} \quad (2.1)$$

Green experimented with the positional dependence of the performance of the absorbers. Measurements were performed with a single absorber placed on the surfaces inside the small cavity shown in Figure 2-2.

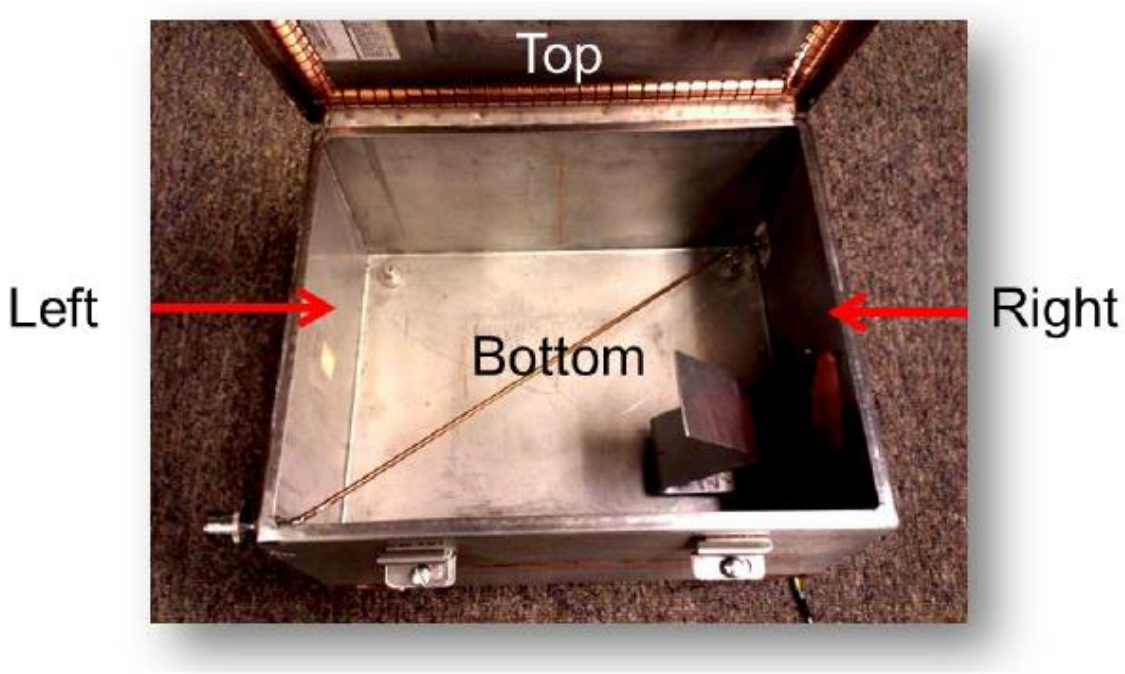

Figure 2-3: Green's Small Cavity Positions[2]

The average S_{21} was measured at these locations with four different materials. At lower frequencies (less than 3 GHz) there was a positional dependence for the *A.E.*, but for higher frequencies the *A.E.* had no positional dependence. This dependence is largely due to the physical dimensions of the cavity and tuner. The cutoff frequency for a rectangular, metallic cavity with dimensions *a*, *b*, and *c*, where $c > a > b$, is calculated using the following equation[3].

$$f_o = \frac{1}{2\sqrt{\mu\varepsilon}}\sqrt{\frac{1}{a}+\frac{0}{b}+\frac{1}{c}} \tag{2.2}$$

Based on the dimensions of the cavity, 15 cm × 25 cm × 30 cm, the cutoff frequency of the cavity in use is calculated to be 781 MHz. Based on [4], the lowest usable frequency to be considered a reverberant environment is triple the cutoff frequency, which is 2.43 GHz. Reverberant environments will be covered in more detail in the next section. In addition to being too low of a frequency to form a reverberant field inside the cavity, the tuner dimensions prohibit the tuner from properly stirring fields below 3 GHz.

2.2 Reverberation Chambers

In Green's work, there was no positional dependence between *A.E.* and absorber placement if the cavity was reverberant. In Richardson's work[5], reverberation chambers are described as a reflective cavity that is electrically large (cavity dimensions much greater than the wavelength of the frequency of interest). In addition to these two physical requirements, there is a time requirement before a space can be considered reverberant after energy is injected into the cavity. Ample time must pass for the energy injected into the cavity to be able to reflect multiple times so that a standing wave pattern can properly form. Richardson defines the average time between reflections as the wall scattering time, T_c, which can be calculated with the following equation:

$$T_c = \frac{4V}{S \times c} \tag{2.3}$$

where

V is chamber volume.

S is chamber surface area.

c is speed of light.

According to Richardson, after 8 to 10 scattering times have passed, the multiple reflections will have constructively and destructively interfered with one another enough times that no specific path dominates the others. When no specific path is dominant, the power received by an antenna will follow a Chi-Square distribution with 2 degrees of freedom (exponential) as long as there is not a direct path between the transmitter and receiver. Figure 2-3 shows an ideal exponential cumulative distribution function (CDF) compared to the CDF of the normalized received power from different tuner positions inside the reverberation chamber at the Naval Surface Warfare Center Dahlgren Division (NSWCDD).

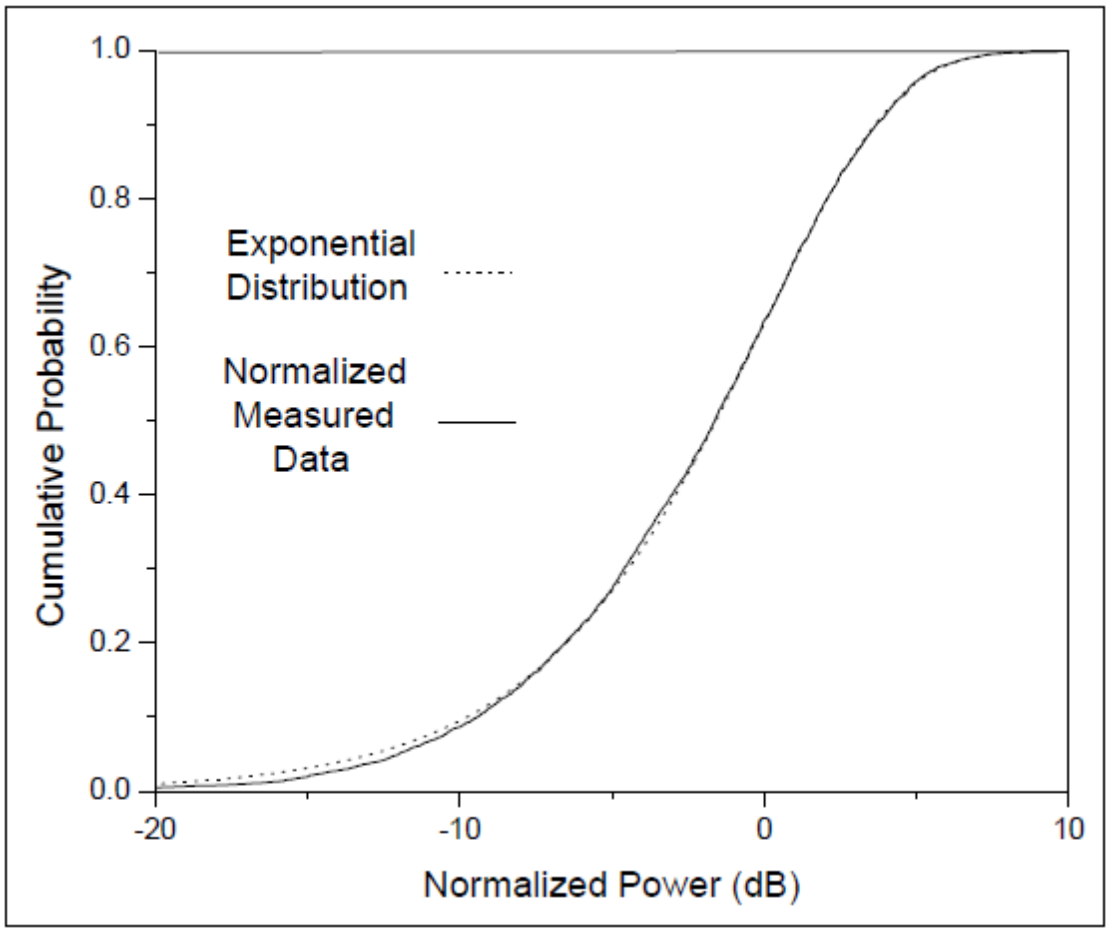

Figure 2-4: Comparison of Ideal and Measured CDF in Reverberation Chamber [5]

The requirement to not allow a direct path does not mean than the two antennas cannot be in line of sight from one another, but merely they must be separated greater than the reverberation distance, which according to [3] is the distance at which the direct path no longer dominates the reflected paths. Rajamani defines the reverberation distance by the following equation:

$$Reverberation\ Distance = \frac{1}{2}\sqrt{D_1 D_2 \frac{4V\omega}{cQ}} \tag{2.4}$$

where

D_1 is the directivity of antenna 1.

D_2 is the directivity of antenna 2.

V is the volume of the chamber.

ω is the angular frequency.

Q is the quality factor of the chamber.

c is speed of light.

Beyond this distance, the direct path is no longer dominant and the power received is once again an exponential distribution. It is important to note that those two single measurements in a reverberation chamber will not likely yield the same results, but if enough samples are taken, and the averages are compared, they will be statistically the same. This effect from passing the reverberant distance was prevalent in Green's work when comparing the performance of the absorbers. If the frequency range was high enough for the fields inside the cavity to be reverberant, then there was no positional dependence because of the uniform (positionally independent) nature of reverberant fields. Reverberation is dependent on the frequency range because the fields inside the cavity become the resulting fields from the standing waves formed by being bound between conducting surfaces. Since the surfaces of the chamber are conductive, tangential components of the electrical field are forced to be zero. In order to meet this

requirement, the only waves that a cavity with dimensions $a \times b \times c$ can support are standing waves with frequencies that satisfy the following equations.

$$f_o = \frac{1}{2\sqrt{\mu\varepsilon}}\sqrt{\frac{m}{a}+\frac{n}{b}+\frac{p}{c}} \tag{2.5}$$

where

m, *n*, and *p* are integer multiples of half wavelengths.

These standing waves result in peaks and valleys separated by $\lambda/2$ spacing. In order for the field to be statistically uniform, a large bandwidth is required so that the field at any point does not consistently fall into a peak or null. Typically, bandwidth constraints limit the mode structure from reaching the ideal uniform field. In order to combat this bandwidth limitation, a mechanical tuner is often used to change the mode structure. A new standing wave pattern is created by moving the tuner to a new location. By taking a measurement at many statistically independent positions and taking an ensemble average, a uniform field can be approximated. The design rules and constraints are outlined in [6]. The tuners are not required to be fully constructed out of conductive material, but the outer surfaces must meet this requirement. In order to sufficiently change the boundary conditions, the tuner must be at least 60% of one of the dimensions of the cavity. Also, the size of the tuner must be at least $\lambda/2$ of the lowest desired frequency in order to properly scatter the fields.

2.3 *Q* Measurements

In [2], Green examined how loading a cavity with absorbers affected the *Q* of the cavity. Since the *Q* of the cavity can be measured and it changes with the amount and type of absorbers, comparing the change in *Q* is a simple method for determining the absorbers' effect on the cavity. There are many different methods for measuring the *Q* of a cavity. In [7], Hill derives the following expression for *Q*.

$$Q = \frac{16\pi^2 V}{\lambda^3}\frac{< P_r >}{P_t} \tag{2.6}$$

where

V is the volume of the cavity.

λ is the wavelength of a given frequency.

$<P_r>$ is the ensemble average of the power received.

P_t is the power transmitted.

Keeping in mind that the ratio of the average power received to the power transmitted can be obtained by using a VNA and performing an S_{21} measurement, the Q of a cavity can be measured in the frequency domain with a specific Q value for every frequency. A key limitation of this approach is that it requires the receiving antenna to be impedance matched and lossless. A mismatch correction can be performed to offset the power reflected back due to impedance mismatch. If the antenna's efficiency is known, the loss mechanism can also be accounted for, but this is not a simple characteristic to determine. If a commercial antenna is used, then this information may be available in its datasheet, but in the case of physically small, electrically large cavities it is often unrealistic to use such devices. For instance, in the cavity that was primarily used in this research, small monopole antennas had to be used in order to be able to be placed inside the cavity without occupying the whole volume of the cavity. These monopoles were poorly matched over most of the frequency band, and their efficiencies were unknown. Fortunately, when measuring Q in the time domain, the antenna mismatches and efficiencies are removed from the measurement [8]. Richardson derives a time domain based expression for Q in [5].

$$Q = \omega\tau \tag{2.7}$$

where

ω is the center frequency of the pulse

τ is the chamber time constant

τ can be calculated using the following equation.

$$\tau = \frac{4.3429}{slope(\frac{dB}{\mu s})} \tag{2.8}$$

Figure 2-5 shows an example of two time domain measurements with different loading conditions.

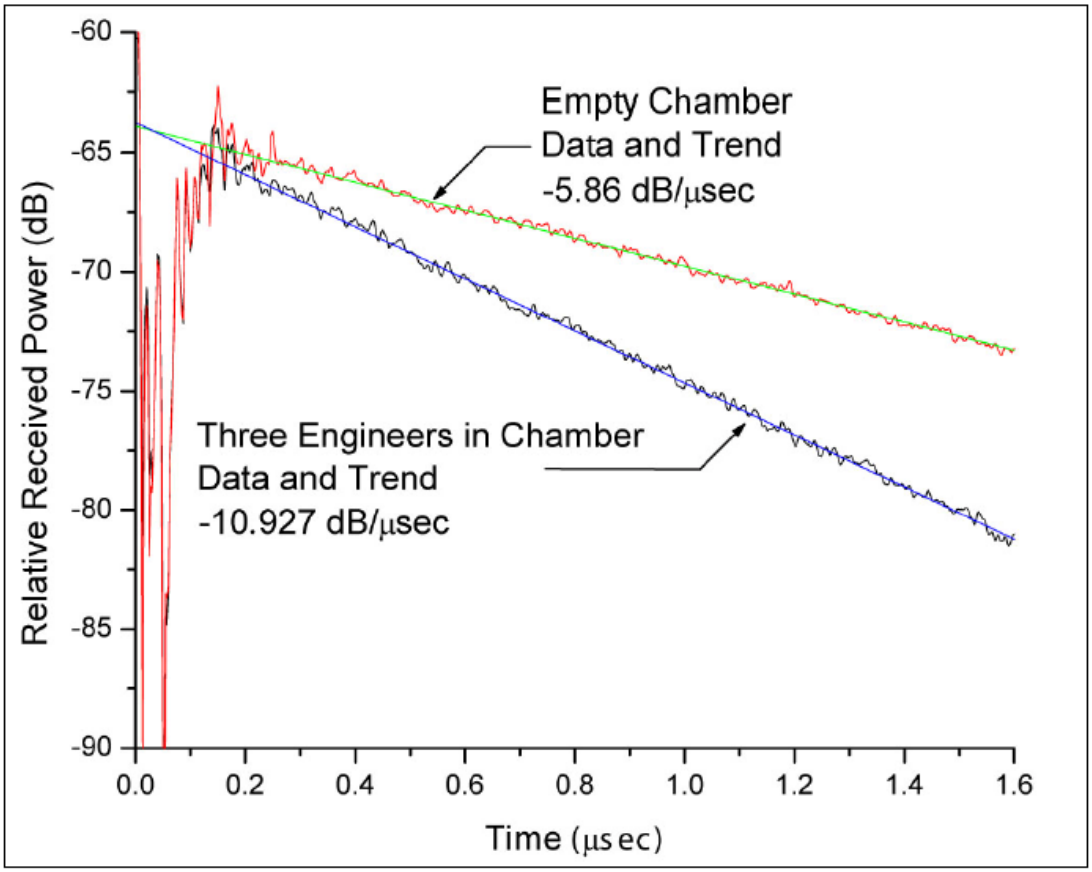

Figure 2-5: Reverb Time Domain Loading Example[5]

By measuring *Q* in the time domain, the impedance mismatch and antenna efficiency do not affect the *Q* measurement [8]. The mismatch results in power being reflected back to the transmitter. The inefficiency of the antenna results in less power being radiated due to the losses. Both of these effects occur before entering the reverberant phase. As a result, they will not change the rate of energy decay. The total power will just begin at a lower starting point while the rate of

decay remains the same. Figure 2-5 demonstrates how the initial reflection from the impedance mismatch is unaffected by the loading inside the chamber. The two pulses are aligned until approximately 0.15 μs, which is the time in which the initial reflection due to mismatch occurs as well as the pre-reverberant phase where the waves are initially scattering around the cavity. However, after entering the reverberant phase, the two signals clearly diverge from one another showing the impact that the loading has on the slope, which is the rate of decay. Unfortunately, performing measurements in the time domain is not an easily accomplished task. In [9], Green outlined a method for measuring *Q* in the time domain using a VNA as with the frequency domain measurements, but by utilizing a time domain transform feature, it was possible to emulate a time domain signal. The VNA captures data in the frequency domain, and performs an Inverse Fourier Transform (IFT) to calculate the magnitude response in the time domain. The key limitations result from the large bandwidth requirement of the time domain *Q* method, which Green derives from the maximum allowed pulse width. Green assumed that the pulse width of the signal was required to be shorter than the wall scattering time so that energy was not still being injected into the cavity when the rate of decay was being calculated. In order to achieve a short pulse width, a wide bandwidth is required. Green initially utilized a two port time domain approach. Figure 2-6 shows an illustration of a wave traveling through the cavity under the two port approach.

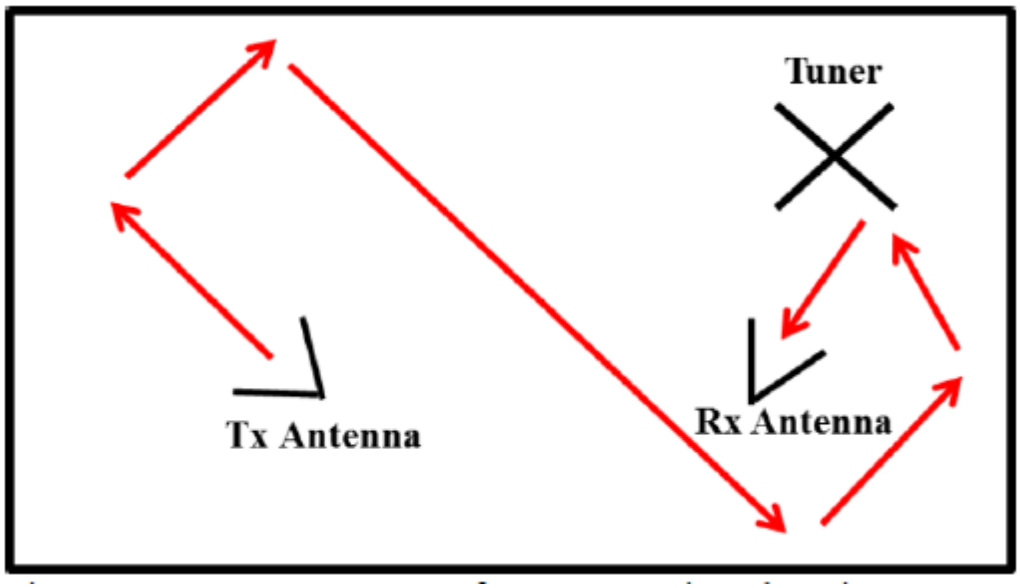

Figure 2-6: 2 Port Wave Illustration[9]

From this illustration, it can be seen that a wave can reflect around the cavity until it is received by the second antenna. Green then hypothesized that a lone antenna could be used as the transmitter and receiver, similar to many radar systems, and the wave could take a path similar to the one illustrated in Figure 2-4.

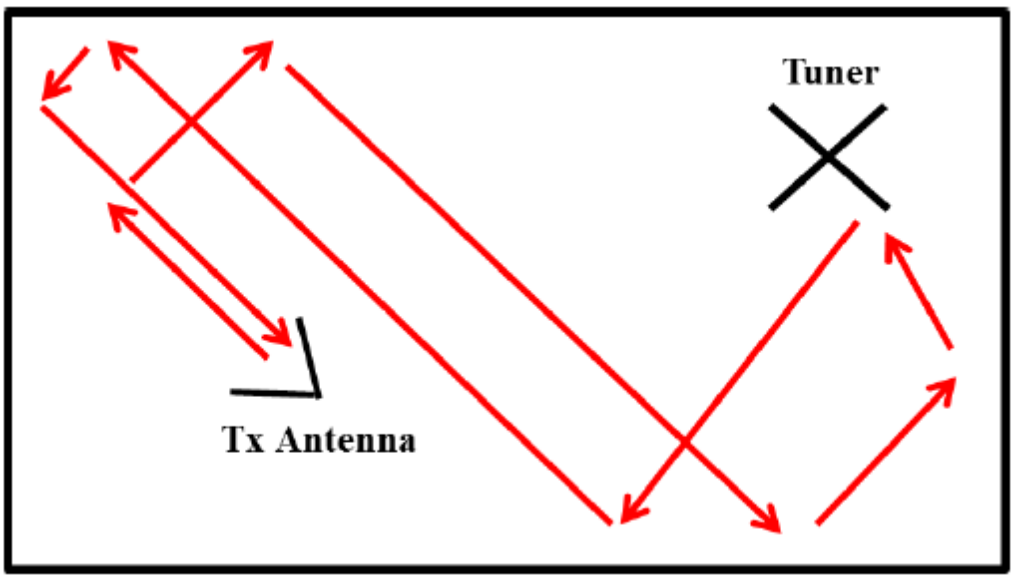

Figure 2-7: 1 Port Wave Illustration[9]

His control experiment was performed inside an ETS-Lindgren SMART 80 Chamber using well-matched Dual Ridged Horn Antennas. Multiple frequency bands were tested with both the one and two port time domain approaches. Both values were compared to one another as well as the *Q* values calculated using the frequency domain approach. The final results indicated that there was a very strong agreement between the one and 2 port approaches. There was at most a 0.70 dB difference between the two values. It is worth noting that the frequency domain *Q* was typically 1-2 dB lower than the time domain *Q* results. The one port *Q* values were consistently higher than the two port values, but this was decided to be a result of having one less antenna loading the cavity.

2.4 Emissions Measurements

When determining the likelihood of a device to cause EMI with other devices, it is important to have a reliable method for determining the amount of power that radiates from the device. It is possible to simulate the device, but due to the varying complexities from one product to the next, such as PCB layouts, interconnections, and structural modifications, simulation can be virtually impossible to account for all of these minor differences. A measurement approach is much more practical. In [10], test procedures are outlined for emissions measurements. There is a procedure for testing the device in an anechoic environment as well as a procedure for testing in a reverberant environment. The anechoic approach has a rigorous setup. There is an initial measurement performed with a known device to provide a baseline. An illustration of the test setup can be seen in Figure 2-8.

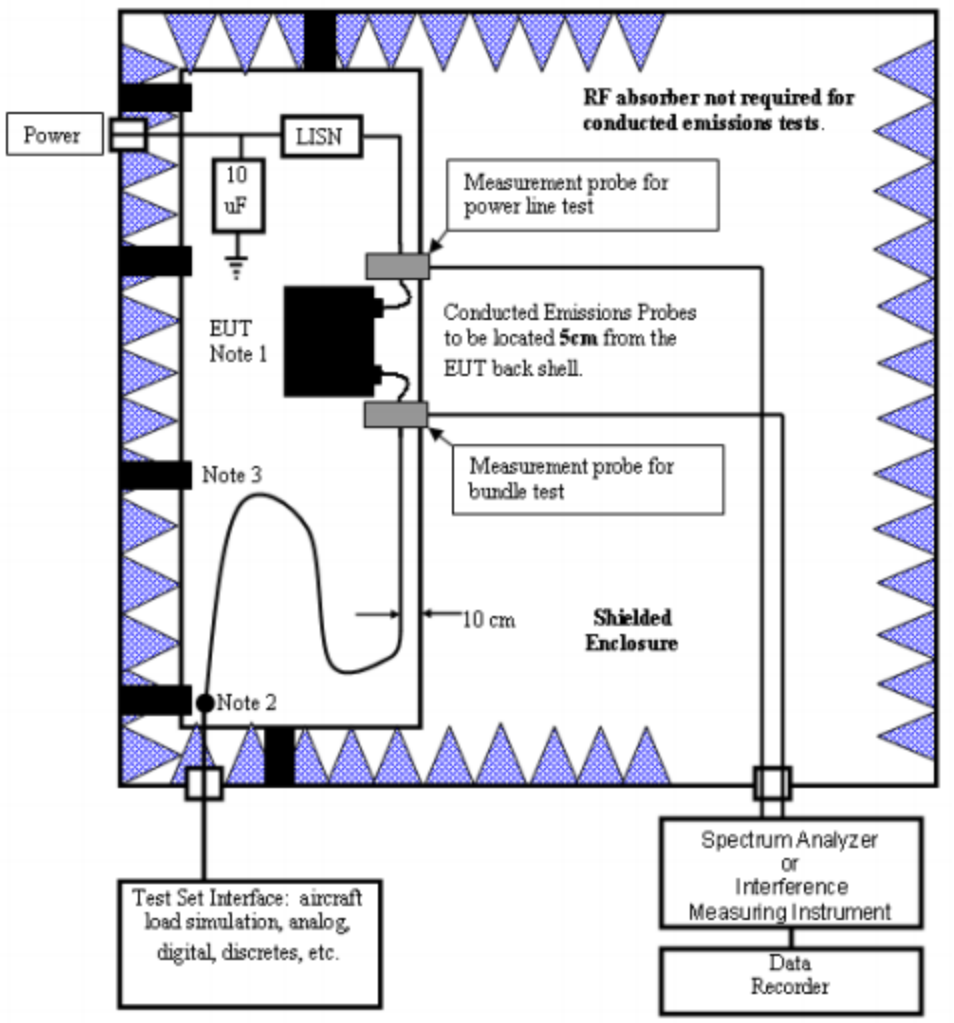

Figure 2-8: Anechoic Emissions Measurement Setup [10]

The receiving antenna must be 0.3 m above the ground plane. The receiving antenna must be 0.9 m from the aperture of the device. The cables must be 10 cm away from the walls of the test device and run parallel to the walls for less than 1 m. RF absorbers must be above, behind, and on both sides of the test setup. The absorbers must extend more than 50 cm in front of the ground plane, and the distance between the receiving antenna and the absorbers must be greater than 30 cm. The receiving antenna must be linearly polarized. Measurements must be performed from multiple angles of each aperture in both polarizations. After this laborious setup, the measurement

uncertainty can still range from 3.5 dB up to 11 dB [4]. The alternative reverberant approach has a much less rigorous setup. Since directivity and orientation do not matter provided that the device is in the working volume and separated by the reverberation distance, the only requirement is that an adequate number of samples are taken over the full tuner rotation. In [11], Koepke and Ladbury outline a procedure known as the substitution method. This is a method for measuring the emissions from a device by first measuring the power received from a known device, then measuring the power received from the test device and using the two values to determine the power transmitted from the test device. A simple example would be if a known transmitter was used and the average power received was -35 dBm. When the test device is used, the received power is -50 dBm. The *Q* of the cavity, as defined by equation 2.6, is a constant value at a given frequency, and therefore the ratios of power received to power transmitted have to remain the same. As a result, it can be deduced that the power emitted from the test device is 15 dB lower than the power transmitted by the known device. Due to the statistical nature of reverberation chambers, they provide a more reliable emissions result than the anechoic approach. Since the directivity and polarization do not affect the results, the setup for reverberation experiments is much less rigorous than the anechoic measurements.

2.5 Summary of Literature Review

This concludes the review of previous work related to this research. While reducing aperture size is an easy method for reducing emissions, it is not always feasible. RF absorbers can be used to accomplish the same goal, but more work is needed to understand how to effectively and efficiently use these materials. Green's work outlined a procedure for measuring the absorber's effect on *Q*, but it has not been verified that reduction in *Q* translates to reduction in emissions. In order to address this, different methods of measuring *Q* as well as emissions were researched. The following chapter will outline the experimental procedures used in collecting *Q* and emissions data in order to determine a correlation.

CHAPTER III

Experimental Methods

This chapter outlines the experimental procedures for collecting the data used in this research. Section 1 will discuss the cavity used for the *Q* reduction experiments. Section 2 will discuss the mechanical tuner used inside the cavity. The first two sections show that the cavity and tuner meet the physical requirements for providing a reverberant cavity at the target frequencies. Section 3 will cover the 2 port time domain technique for measuring *Q* factor. Section 4 will cover the 1 port time domain *Q* factor measurement. Lastly, section 5 will cover the emissions measurement setups and techniques. The data collected using these techniques is crucial for establishing a correlation between *Q* and emissions.

3.1 The Cavity

The cavity used for these experiments was a rectangular, metal box with dimensions of 0.25 m × 0.15 m × 0.3 m. Figure 3-1 shows the cavity as it was before any modifications were performed.

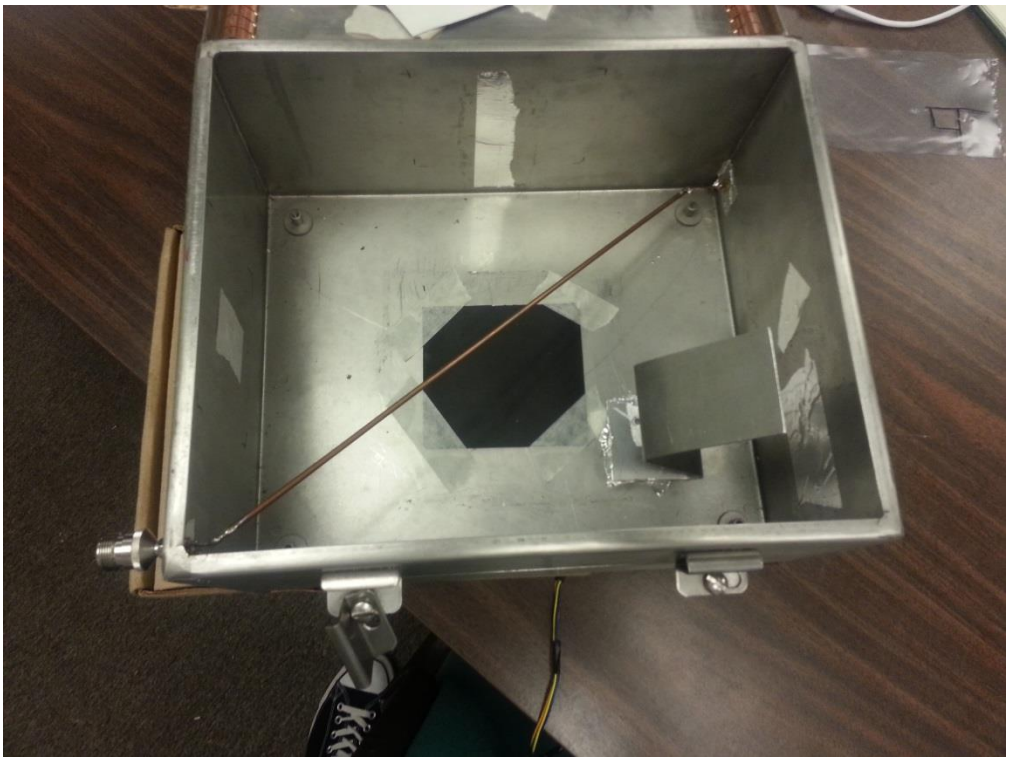

Figure 3-1: The Test Cavity with Original Probe

The cavity originally had a diagonal probe that ran from the front top left corner of the cavity to the back bottom right corner of the cavity (from the perspective of the above picture). Each end of the probe was connected to an SMA connector. One SMA connector was coupled to an N-type adapter so that it could be connected to the appropriate RF equipment (VNA, Spectrum Analyzer, Signal Generator), and the other was terminated with a 50 Ω load. The probe was 0.368 m in length and ran directly through the usable volume of the cavity. A large portion of the working volume could be affected by the near field effects of the probe since it runs diagonally through the cavity. In order to minimize these effects, this probe was replaced by two monopoles designed for operation at 2 GHz. Figure 3-2 shows the cavity with the new monopoles.

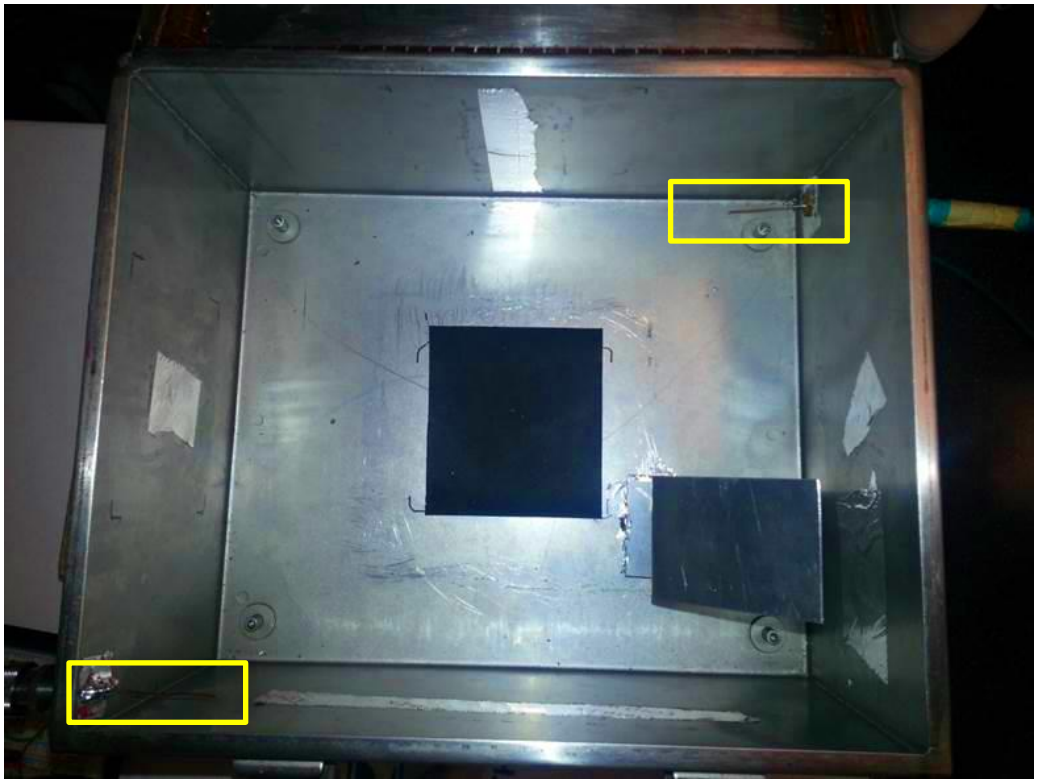

Figure 3-2: Test Cavity with New Monopoles

Attaching the 2 monopoles allows for 1 and 2 port measurements to be performed inside the cavity whereas before only a 1 port measurement could be performed. In order to perform a 2 port measurement before, a nested cavity approach was required which results in increased experiment time due to the need to properly stir the outer cavity.

3.2 The Tuner

Inside the cavity, there was a z-fold tuner attached to a stepper motor. As discussed in Chapter 2, this tuner provides a method to mechanically stir the environment to achieve a statistically uniform field. The tuner was 12.75 cm tall. This length was 85% of the height of the chamber and well over the minimum requirement of 60% as explained in [6]. The width of the tuner was 5 cm which was the half wavelength of 3 GHz. As a result, the lowest frequency sufficiently stirred was 3 GHz.

3.3 2 Port Time Domain *Q* Factor Measurements

In the 2 port time domain technique for *Q* measurements, one antenna was used as a transmitter while the other antenna was used as the receiver. The ratio of the power received compared to the power transmitted, S_{21}, was measured with respect to time. A variant of this method is to use a VNA to measure S_{21} in the frequency domain and perform an Inverse Fourier Transform (IFT) to emulate the usage of a time domain pulse. An illustration of the test setup can be seen in Figure 3-3.

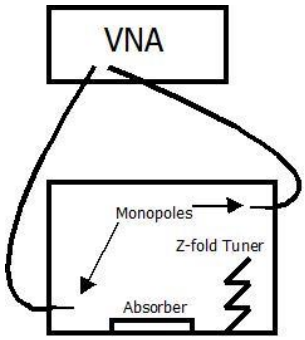

Figure 3-3: 2 Port *Q* Factor Test Setup

In Green's work [9], it was determined that the pulse width of the signal needs to be shorter than the wall scattering time to prevent the measurement being skewed by energy still being injected into the cavity. The cavity used for these experiments was 0.3 m × 0.15 m × 0.25 m which results in a surface area of 0.315 m^2 and a volume of 0.0113 m^3. These values can be used to calculate the wall scattering time based on the work of Richardson [5] using the following equation:

$$\frac{4V}{SA * c} = 476.2\ ps \tag{3.1}$$

Following the work of Green [9], Equation 3.1 gives the maximum pulse width because the pulse width needs to be shorter than the wall scattering time. The premise of this assumption was that if energy is still being injected into the cavity, the measured rate of decay would be skewed. For the VNA used in these experiments, the Agilent 8722ES, the pulse width was calculated using the following equation which can be found in an Application Note for this device[12].

$$Pulse\ Width = \frac{2 * 0.98}{Bandwidth} \tag{3.2}$$

By combining equations 3.1 and 3.2, the minimum bandwidth required was calculated to be 4.12 GHz. As a precaution, a bandwidth of 5 GHz was chosen for these measurements. In Chapter 4, the requirement of this bandwidth is contested. The VNA was set to the target center frequency, 5.5 GHz, with a span of 5 GHz, and the number of points was set to the maximum value of 1601. A calibration of the VNA was performed to remove the effects of the cables from the measurements including the time to propagate through the cables and any impedance mismatch from the cables. This standard two-port calibration consisted of terminating both cables with an open connector, a short connector, and a broadband 50 Ω load. The final calibration measurement was performed by connecting the two cables together for a through measurement. After completing the calibration, the cables were connected to the N-type ports on the cavity, and the door was closed and clamped shut. The S_{21} data was recorded, and the tuner was incremented to the next position. S_{21} data was recorded at every tuner position until the tuner made a full revolution (which was 50 steps of 7.2 degrees for these experiments). Initially, it was required to manually increment the tuner and save the data at each location, but a LabVIEW Virtual Instrument was used to save the S_{21} data then increment the tuner. As a result, the user only had to

interact with the experiment every 5 minutes rather than every 6 seconds. After performing a few measurements, it was determined that the user could perform a calibration for each desired frequency band and store each calibration into a register on the VNA and the LabVIEW VI was then modified to receive a user input of how many states to run. Rather than performing 50 measurements for each tuner position and then requiring the user to switch to the next calibration, the VI would repeat the process for the desired number of experiments. This change meant that the user only has to interact with the experiment every hour to change the loading rather than every 5 minutes from the previous version of the VI.

3.4 1 Port Time Domain *Q* Factor Measurements

Following the work of Green [9], the experiments performed in the 2 port time domain measurements were repeated using only a single antenna. The benefits of using a single antenna include cheaper costs, simpler setup, and there was much less volume occupied by a single antenna. Under this setup, the lone antenna was both the transmitter and the receiver. In this setup, the S_{11} measurement was performed, which was the ratio of the reflected power at port 1 relative to the incident power at port 1. The premise was that the power received was still proportional to the energy in the cavity regardless of the number of antennas. An illustration of the test setup can be seen in Figure 3-4.

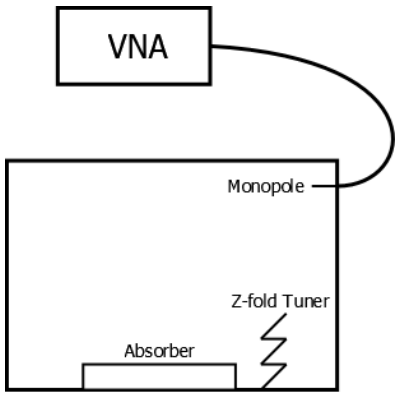

Figure 3-4: 1 Port *Q* Factor Test Setup

With the exception of which S parameter was being measured and the corresponding VNA calibrations, all other steps of the experiment remain the same.

3.5 Emissions Measurements

In order to address the primary objective of this research, a test procedure for measuring the maximum emissions needed to be established. Normally a device being tested follows the testing procedure outlined in [10]. While this setup could be performed, a more rigorous approach was used. The test cavity was placed inside the ETS-Lindgren SMART 80 chamber. The tuner inside the cavity and the vertical tuner in the SMART 80 chamber were continuously stirred. A monopole inside the cavity was connected to an Agilent E8257D signal generator to act as a source, and a Dual Ridged Horn Antenna, DRHA, was placed in the SMART 80 chamber and connected to an Agilent E4407B Spectrum Analyzer to act as a receiver. The Spectrum Analyzer was set on a max hold sweep, which will retain the highest value measured for a given frequency over a specified duration of time. The tuner inside the cavity rotates with a period of 16 s and the tuner in the SMART 80 chamber rotates with a period of 29s. The sweep time varied between experiments, but was not less than the fundamental period of the two tuners (7m 44s). After this

amount of time, all combinations of the tuner positions are achieved and further measurements are redundant.

An alternative approach for measuring the emissions was developed based on [11]. This setup still requires a nested cavity approach, but rather than the initial "reference measurement" being performed with a transmitter that has known characteristics and the subsequent measurements performed with an unknown device, the initial measurements are performed with an empty nested cavity and the subsequent measurements are performed under different loading conditions for the nested cavity. Based on the S_{11} parameters of the monopole inside the cavity, the monopole radiated less than half of the power transmitted. The mismatch of the monopole does not play a factor in the time domain Q measurements[8], but for the S_{21} measurements in the frequency domain a better matched transmitter was required. As a result of these considerations, a different cavity was required for the emissions measurements. This new cavity has dimensions of 76.2 cm × 122 cm × 213 cm. This larger chamber allowed for the use of another DHRA as the transmitter which allowed much more power to be coupled into and out of the cavity. A picture of the new cavity can be seen in Figure 3-5.

Figure 3-5: Senior Design Chamber Inside SMART 80

This cavity had two 30 cm × 30 cm windows that were originally covered with wire meshes installed to provide EM shielding. The wire meshes were removed and Styrofoam blocks were cut to fit and placed into the window openings. The windows were then blocked off with aluminum conductive tape. An aperture of 5 cm ×15 cm was left uncovered in one of the windows to allow energy to radiate. The previous VI was modified to work with the motor controller for the new cavity as well as the tuner inside the SMART 80 chamber. If the user was performing a Q measurement, the VNA was set to measure S_{11} in the time domain, and the tuner inside the small cavity was incremented 49 times to complete a full rotation. If the emissions measurement was desired, then the VNA was set to measure S_{21} in the frequency domain, the tuner in the smaller cavity was incremented 49 times, the tuner in the SMART 80 chamber was incremented by a single 7.2 degree step, and this was repeated until the tuner in the SMART 80 chamber completed a full rotation. This results in 2,450 S_{21} measurements per emissions test.

The following chapter will discuss the performance of these techniques by comparing and contrasting the performance of these techniques as well as discussing the findings of the experiments in which these techniques were used.

CHAPTER IV

Experimental Results and Analysis

This chapter discusses the results of the experiments performed in this research. Section 1 discusses the results of the initial 2 port time domain *Q* factor measurements. Section 2 discusses the results of the initial 1 port time domain *Q* factor measurements as well as a comparison with the 2 port results. Sections 1 and 2 are integral in understanding how the *Q* values are calculated in the later experiments. Section 3 discusses the results of an experiment designed to look at the absorber surface area compared to the absorber volume. Section 4 investigates the effectiveness of the absorber cross section vs volume. Section 5 examines the impact of absorber location relative to each other. Section 6 compares the performance absorbers with a smooth surface against absorbers with a ridged surface. Sections 3 through 6 explore different ways to manipulate the *Q* of the cavity with the goal of finding the maximum reduction with the minimum material. Section 7 investigates the bandwidth requirements of the time domain *Q* factor techniques. Section 7 serves to address concerns regarding the assumed large bandwidth requirement and to determine the validity of the bandwidth limitation. Section 8 discusses the results of the maximum emissions technique. Section 9 discusses the results of the average emissions technique and compares change in emissions from a cavity to the change in *Q* of the cavity in order to determine the correlation.

.

4.1 2 Port Time Domain *Q* Factor Results

By calculating *Q* for any particular loading scheme, there is a fast and reliable method to quantify the amount of absorption that results from loading the chamber by calculating the change in *Q* compared to the empty chamber. Using the 2 Port Time Domain Technique, the *Q* values measured over 12 frequency bands with center frequencies ranging from 5.5 GHz to 11 GHz in 500 MHz increments for the following 4 loading scenarios:

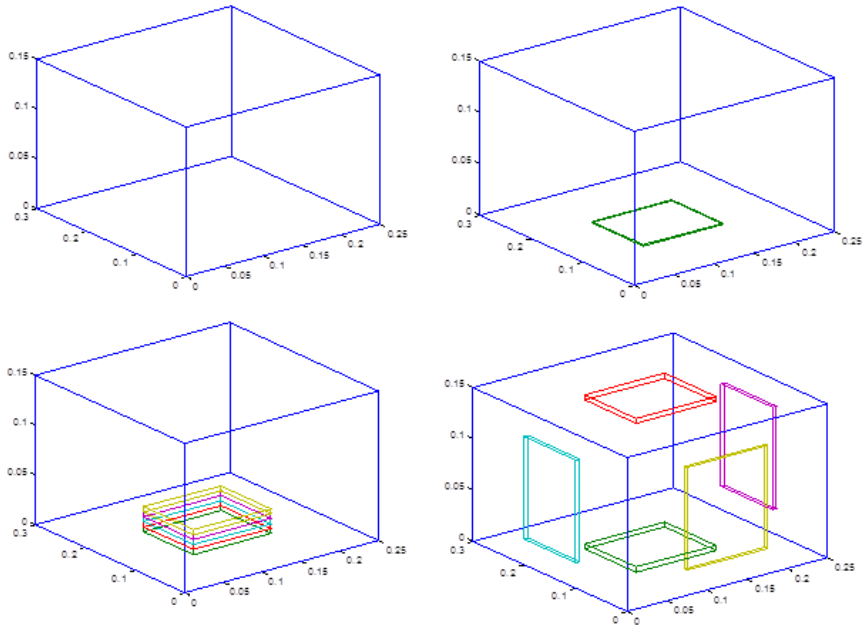

Figure 4-1: Absorber Placement for Different Loading Conditions

The top left is just an empty chamber (further referred to as Empty). The top right has a single absorber on the floor (further referred to as Floor). The bottom left has 5 absorbers stacked on the floor (further referred to as Stacked). The bottom right has 5 absorbers placed on 5 different surfaces (further referred to as Spread). Figure 4-2 shows a sample plot of the S_{21} data measured for an empty cavity at a center frequency of 5 GHz.

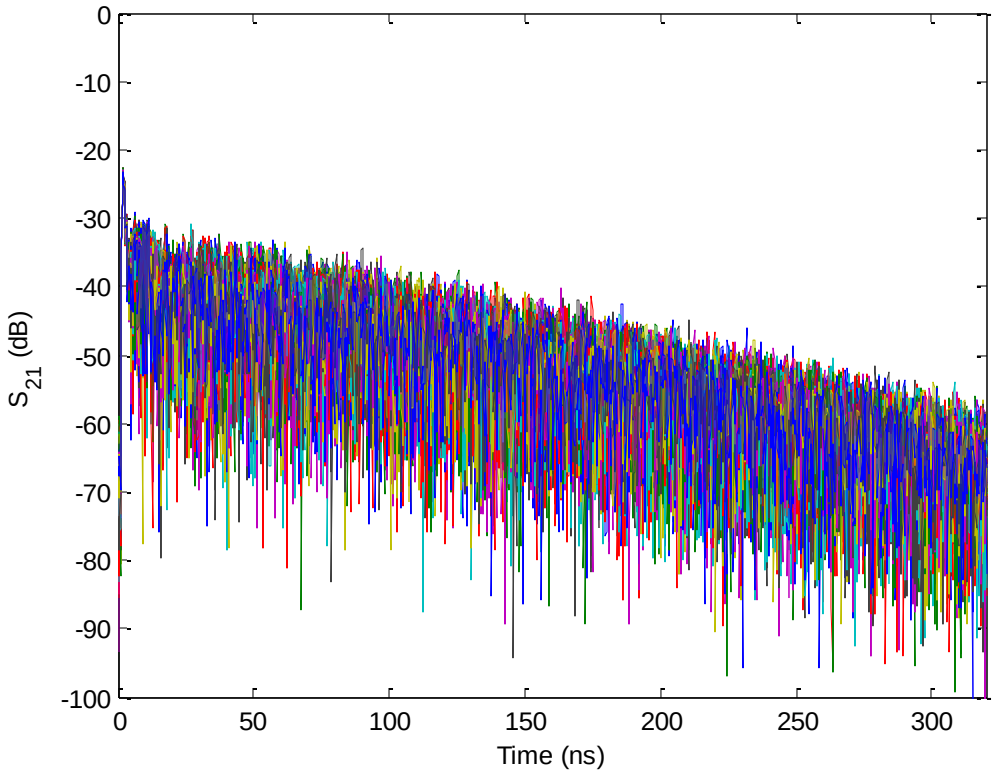

Figure 4-2: S21 Time Domain Measurement Example

It is clear from Figure 4-2 that S_{21} varied greatly from position to position, but the average decay is the desired information. In order to find the overall trend, an ensemble average is taken for all tuner positions. Figure 4-3 shows an example of the ensemble average S_{21} measurement.

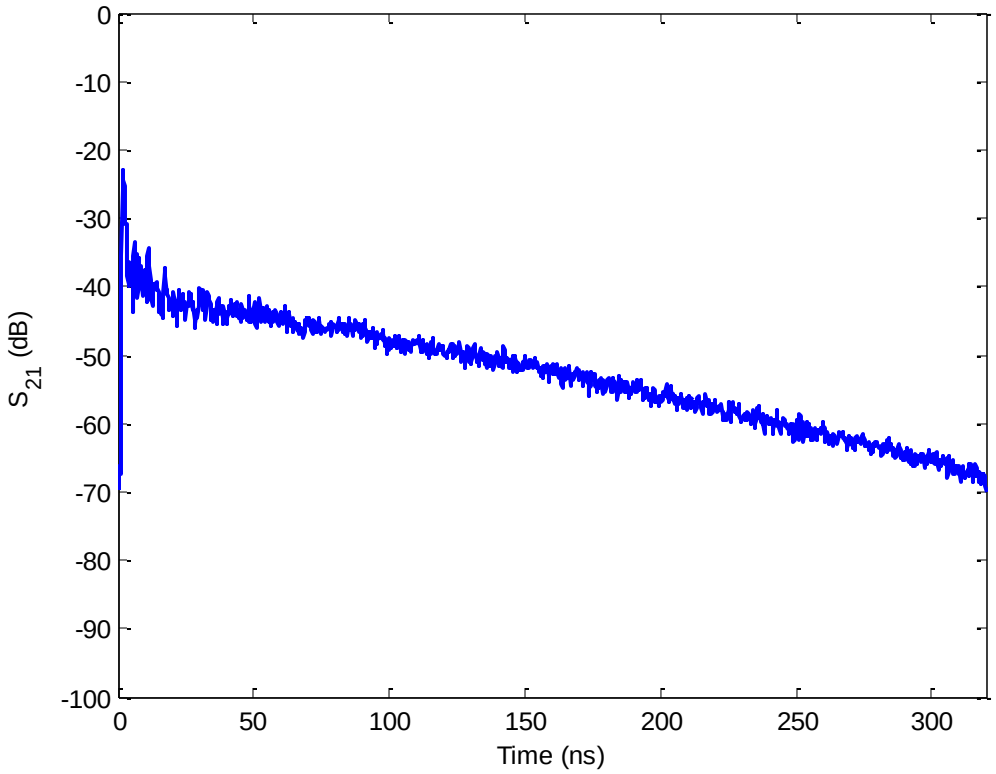

Figure 4-3: S21 Time Domain Average Example

The scattering time of the cavity was 476.2 ps, so the pre-reverberation time only lasts from 3.8 to 4.8 ns. The initial reflection from mismatch can be seen at the beginning where S_{21} jumps up to almost -20 dB, but after about 5 ns, there are no more large fluctuations in the power received. These results follow the same linear trend as in [5] (see Figure 2-3). Figure 4-4 compares the average S_{21} time domain plots for an empty cavity at different frequency bands.

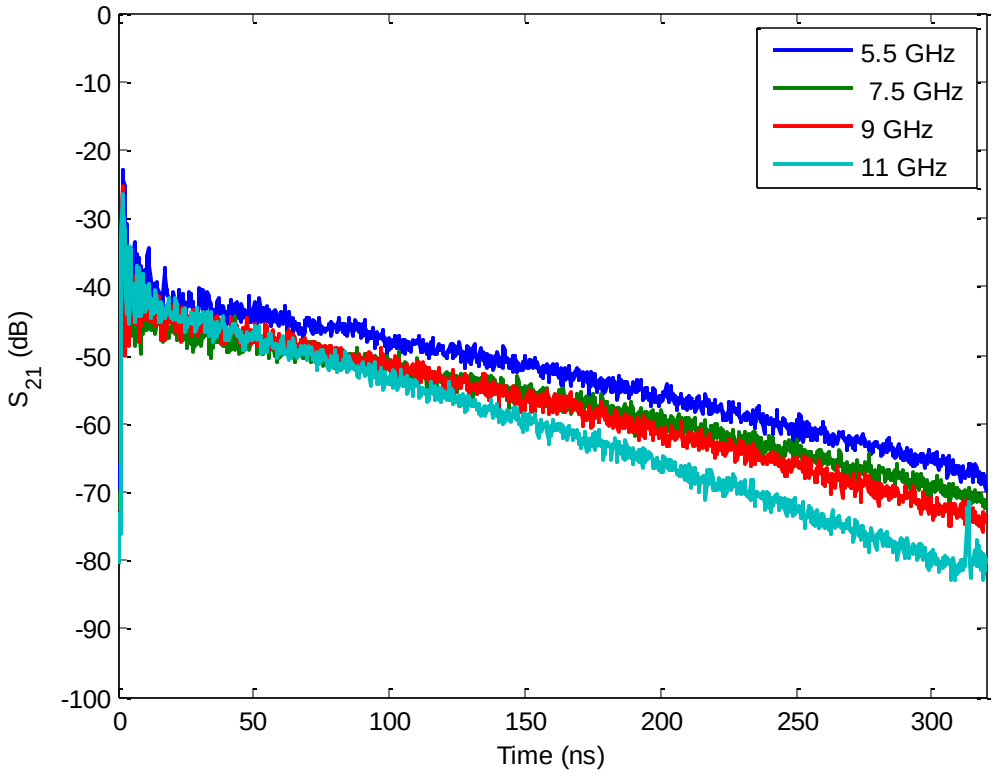

Figure 4-4: Comparison of S_{21} for Empty Cavity at Different Frequencies

For each frequency band, the initial reflection varies slightly, as well as the magnitude of S_{21} at the beginning of the reverberant phase. The initial reflections vary because the reflection coefficients of the antennas change with frequency, and the initial power levels vary because the antennas have different radiation efficiencies at different frequencies. Remember, the important information is not the magnitude of the reflection or the initial values, but rather the rate of decay once the cavity has entered the reverberant phase. A steeper slope indicates that there is more loss in the cavity at that frequency band. For the case of the empty cavity, the only loss mechanism is from electric losses of the walls and tuner. As the center frequencies change, so do the slopes. This is expected because the skin depth, δ_W, is defined as:

$$\delta_W = \frac{1}{\sqrt{\pi f \sigma \mu}} \tag{3}$$

where

f is the frequency.

σ is the conductivity of the material of the walls at the given frequency.

μ is the permeability of the material of the walls.

As the skin depth decreases, the effective resistance increases. If currents with equal magnitude are induced on the walls, the power dissipated will increase with frequency since power dissipation is equal to the square of the current times resistance. Similarly, Figure 4-5 shows the changes in S_{21} when the frequency is kept constant, but the loading is changed.

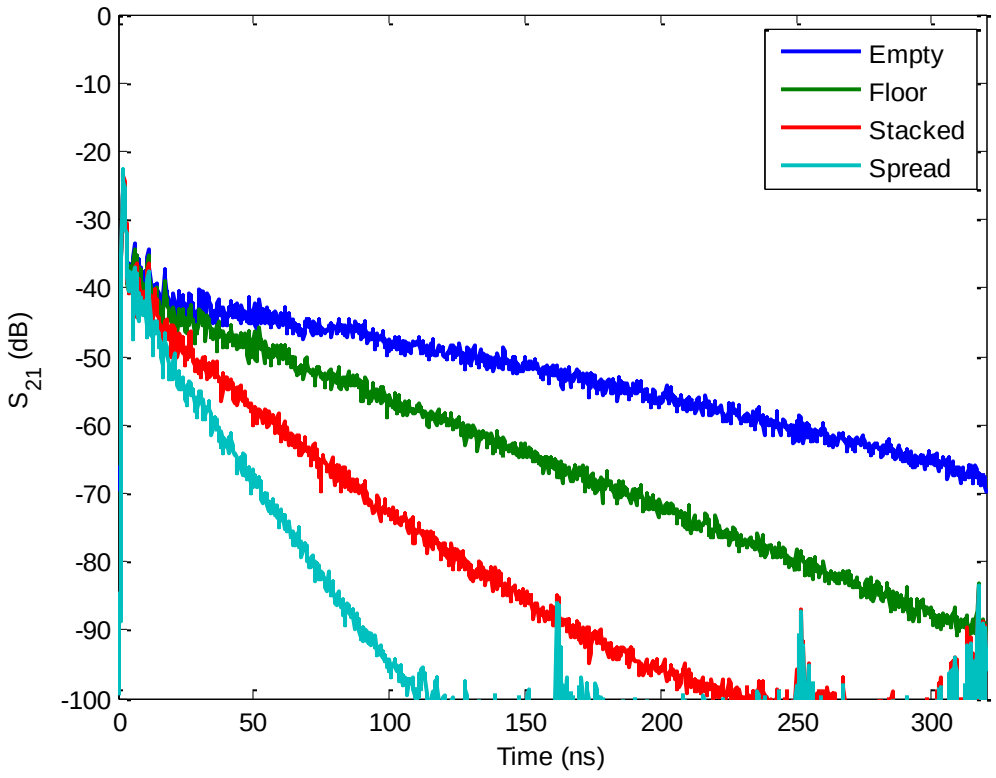

Figure 4-5: Comparison of S_{21} at 5.5 GHz Under Different Loading Conditions

Unlike Figure 4-4, where the only losses were due to the chamber walls, there is a clear distinction between the slopes of the different loading scenarios. Since the frequency was kept the same, it was expected that initially (<4 ns) the plots will align because this portion of the plot is due to the initial reflection, which is the same for each measurement if frequency is constant. However, once the reverberant stage is reached, the loss associated with each loading setup dominates the behavior. The Empty, Floor, and Stacked plots behave as expected. Empty has the lowest slope, which is expected since the only losses are the conductive losses in the chamber. Stacked has a steeper slope than Floor, which is intuitive because Stacked has 5 times the amount of absorbers than Floor. Spread begins as expected. Spreading the absorbers greatly increases the surface area while using the same volume of absorbers as Stacked. The only part of the plot that is unexpected is the spikes that appear for the Spread plots and partially for the Stacked plots. These are a result of using such a large bandwidth (5 GHz). This large bandwidth results an increased noise floor in the frequency domain. This increase in noise levels shows up in the time domain as these spikes. They are all below -80 dB. As a result, -80 dB is considered to be the noise floor for these measurements. While it not difficult to determine the differences which curve has a steeper slope, it is more desirable to have a single quantifiable number for comparing the performance of these absorber setups. Slopes can be calculated (in dB/μs) for the linear portions of the plots. These slopes can be used to find the chamber time constant, τ, using the following equation that follows the work of Richardson [5]:

$$\tau = \frac{4.3429}{Slope(\frac{dB}{\mu s})} \tag{4}$$

In order to calculate τ, a line of best fit is calculated from 20 to 80 ns. This range is chosen to prevent the results from being skewed by the initial reflections or after the energy is attenuated below the noise floor. Once τ is calculated, *Q* can be calculated with the following equation:

$$Q = 2\pi f_c \tau \quad (5)$$

The resulting Q values for each frequency band and loading combination can be seen in Figure 4-6.

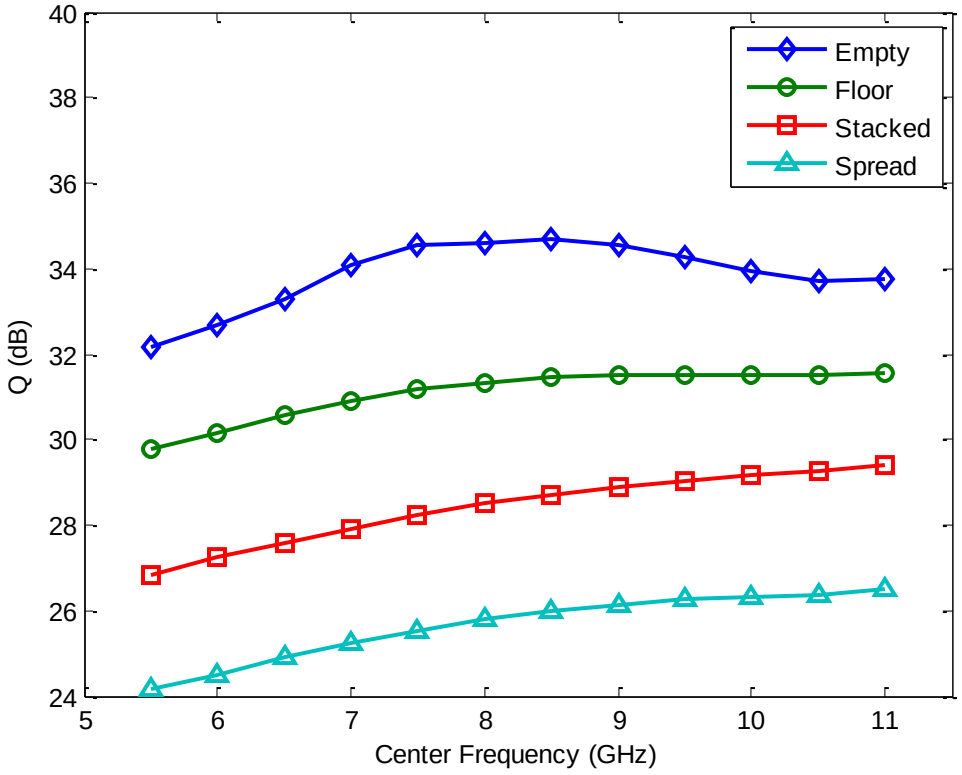

Figure 4-6: Resulting *Q* Calculations from 2 Port Technique

The Q values have very clear separations from one loading setup to the next. There is a decrease in Q of approximately 2-4 dB from placing the first absorber on the floor of the cavity. There is only an approximately 2.5 dB more reduction in Q by increasing the thickness of the absorber 5 times, but when the absorbers are spread out, there is an additional 2.5 dB reduction. This shows that there are diminishing returns on stacking the material and spreading is the better choice if the objective is to reduce Q.

4.2 1 Port Time Domain *Q* Factor Results

The 1 port approach was established in Green's work. In order to validate the technique, the *Q* values for the same loading setups as the previous experiment. An example of the S_{11} data collected from the empty cavity at 5.5 GHz can be seen in Figure 4-7.

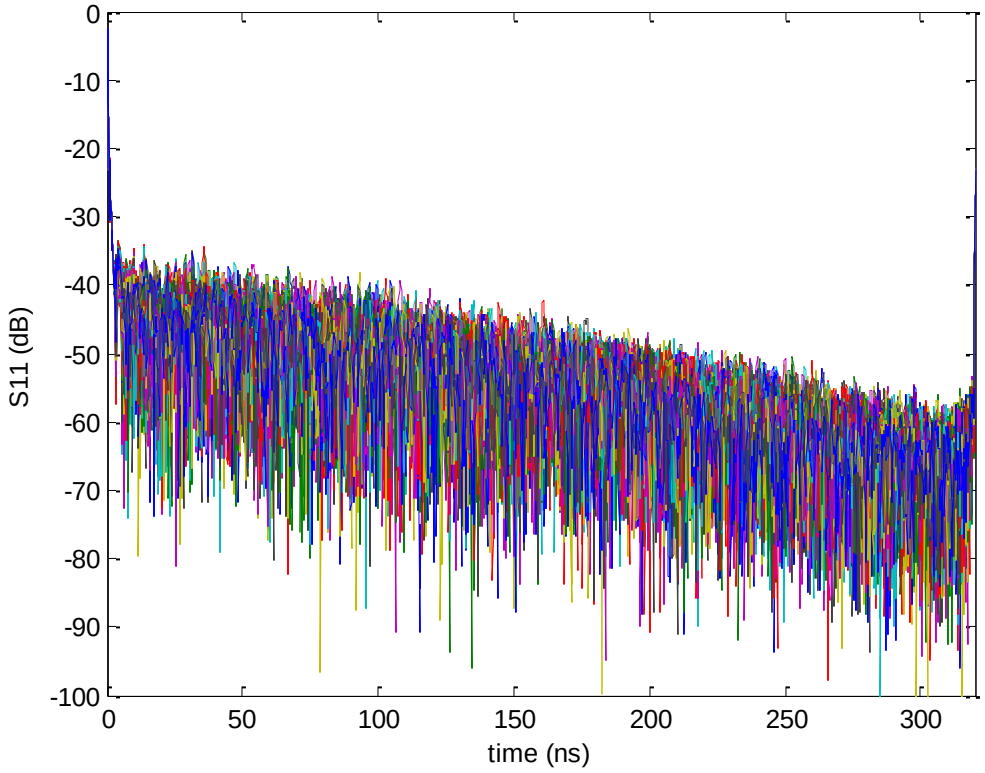

Figure 4-7: S_{11} Time Domain Measurement Example

Similar to the S_{21} measurement, the S_{11} measurement varies greatly with tuner position. As with the S_{21} measurements, an ensemble average is taken so that the plots can easily be compared. The ensemble average of the data shown in Figure 4-7 can be seen in Figure 4-8. The averaged S_{21} data is also plotted for comparison.

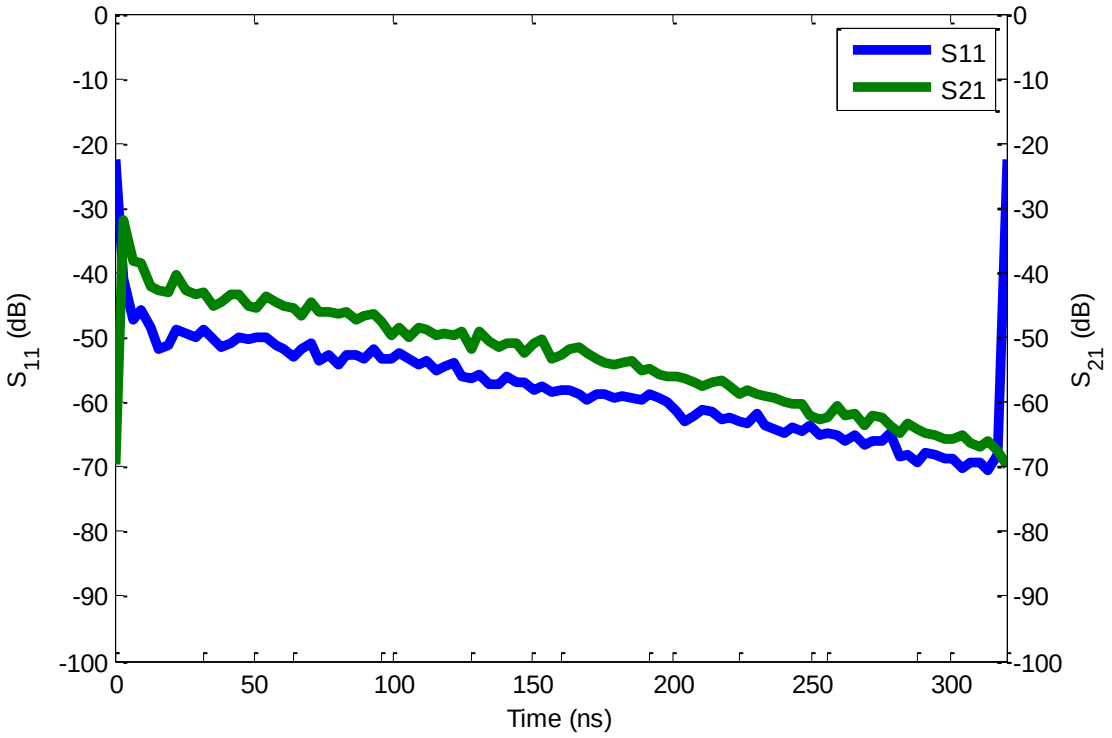

Figure 4-8: S_{11} Time Domain Average Example

The two plots are very similar. Based on this plot, the power received at port 2 is greater than the power reflected back at port 1 since the 2 port values are higher than the 1 port values. The rates of decay are not quite the same. This can be seen because the separation between them when they enter the reverberant phase is less than the separation near the end of the plots. This could be due to the monopoles being so close to the cavity walls. Since the monopoles are not completely placed in the working volume, the fields may be different at each monopole. The purpose of this experiment is not to see how closely the 2 port and 1 port techniques measure *Q* to one another, but rather to see how each technique measures the relative *Q* based on loading. A 1 port *Q* calculation was performed for all 12 frequency bands with the same 4 loading configurations as with the 2 port approach. Figure 4-9 shows the *Q* values measured from the 1 port experiment.

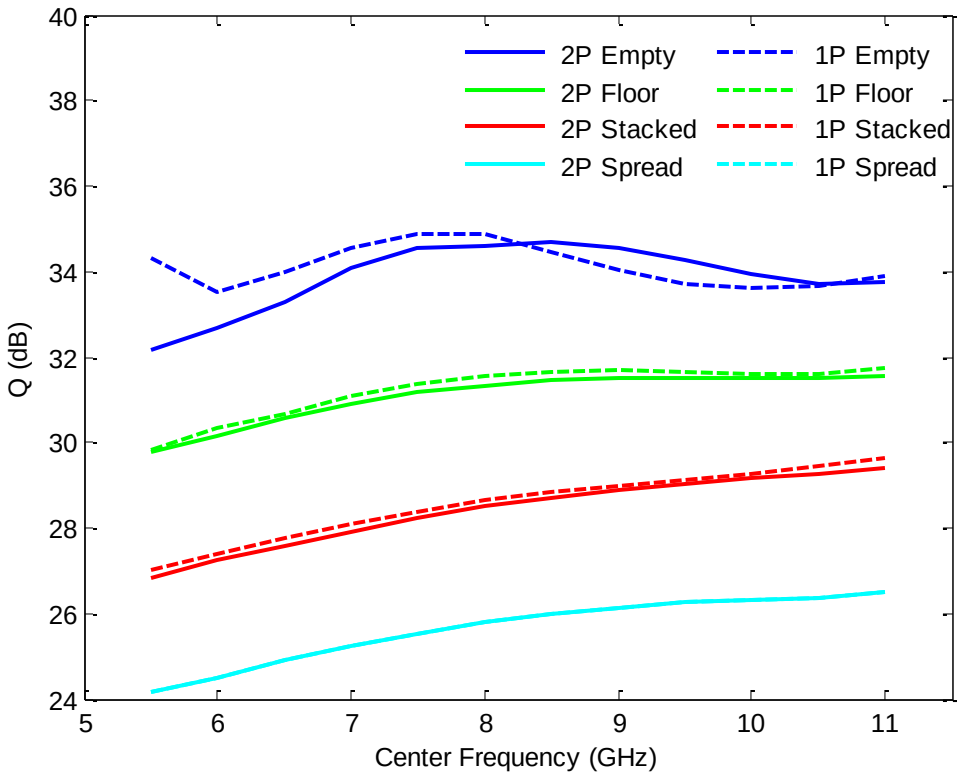

Figure 4-9: Comparison Between 2 and 1 Port *Q* Calculations

Figure 4-9 very clearly shows how closely the 1 and 2 port techniques compare. With the exception of a 2 dB disagreement for the empty cavity at 5.5 GHz, which could have been due to a measurement error, there is virtually no difference between the 1 and 2 port techniques. The 1 port method tends to yield slightly higher *Q* values than the 2 port method, but that is expected based on Green's results. Considering there are no major differences between the results of the two techniques added with the simplicity of the 1 port calibration relative to the 2 port calibration, the 1 port time domain method will be used for all remaining *Q* measurements.

4.3 Absorber Volume vs Absorber Surface Area

The results of both the 1 port and 2 port time domain *Q* measurements indicated that spreading absorbers performs better than stacking them. In order to determine if this was a property of the

EFIG-020 material, the experiment was repeated using WXA-010. Figure 4-10 shows the resulting *Q* values from the WXA experiment.

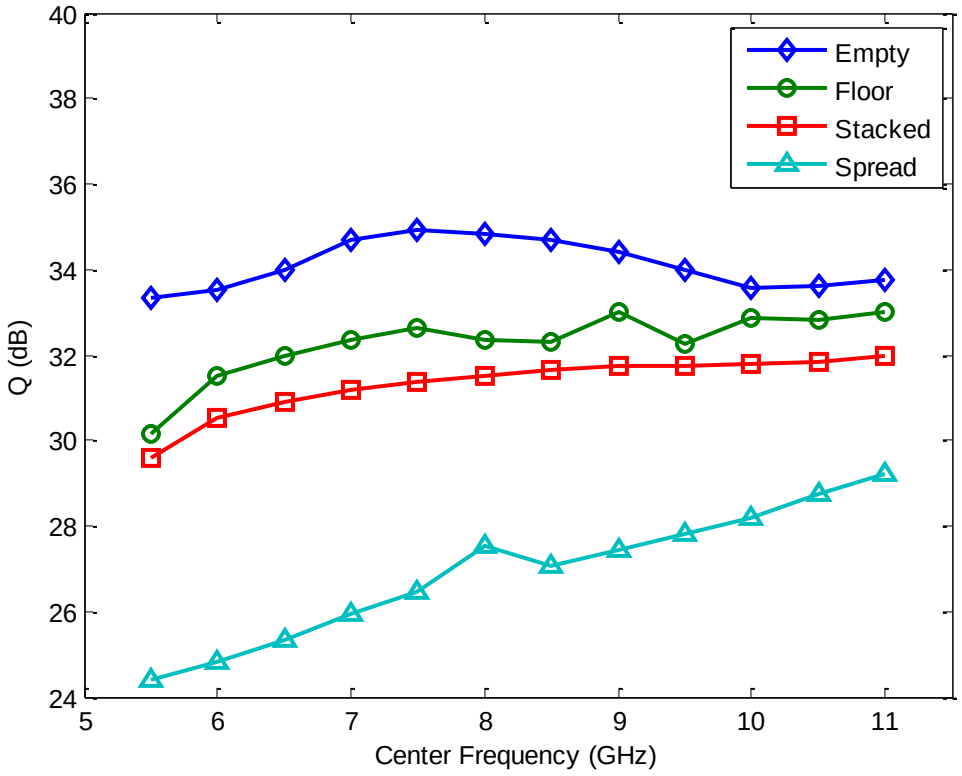

Figure 4-10: WXA *Q* Results

Similar to the EFIG material, there was an initial reduction of 0.75 to 3.18 dB. This indicates that the WXA material performs much better at lower frequencies. The increased performance from stacking the pieces is very small. The decrease in *Q* from Floor to Stacked only ranges from 0.55 to 1.30 dB. Spread, however, has a significant reduction in *Q*. The reduction in *Q* from Stacked to Spread is 2.79 to 5.68 dB. In [13], the following expression is presented for *Q*:

$$Q = \frac{3}{2}\frac{V}{S\delta_W} \tag{6}$$

This definition of Q leads to the notion that filling a cavity's volume and covering the reflective surfaces with an absorbing material will both affect the *Q* of the cavity. It would be beneficial to determine whether filling the volume or covering the surface has more impact on *Q*. Another question that arose was whether or not marginal effects were being lost by having such extreme changes in the loading conditions. In an effort to better address this question, the following experiment was developed. Using the same 12 frequency bands as the previous experiments, four different materials were tested under the loading conditions of 1-5 pieces of pieces of material stacked on the floor and 2-5 pieces of material spread on different surfaces. For this experiment, the *Q* value for the empty cavity is subtracted from the *Q* value for the loaded setup so that the values can be easily compared from one experiment to the next. Figure 4-11 shows the results of stacking the sheets of absorbers on the floor of the cavity.

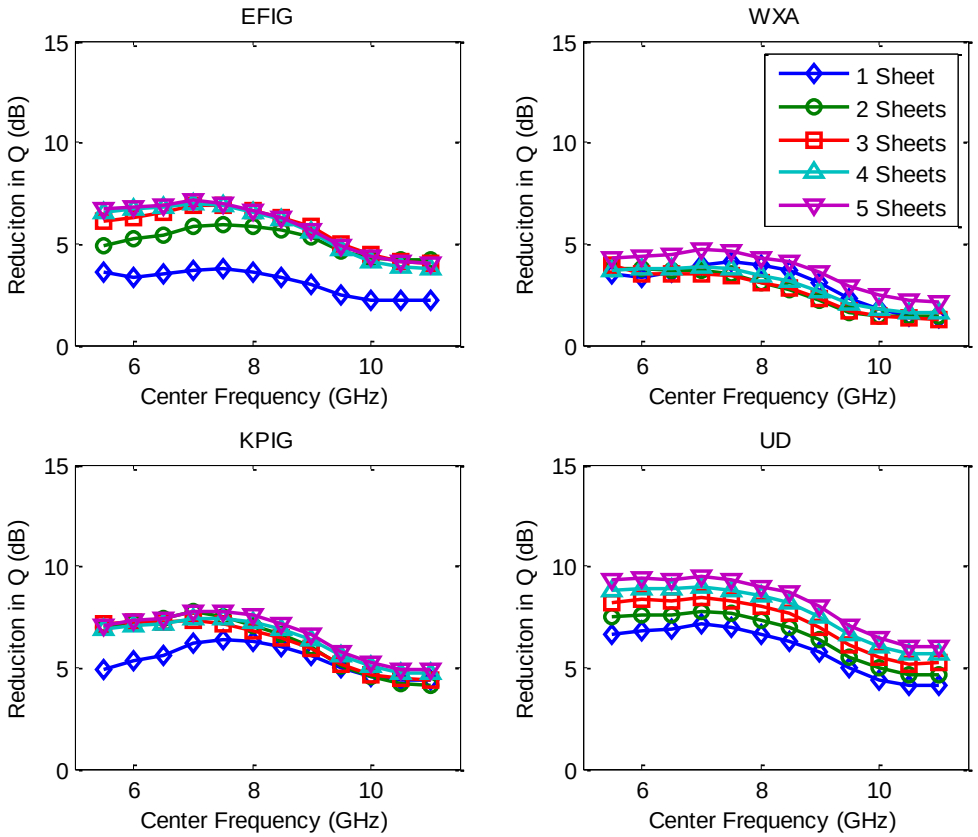

Figure 4-11: Results from Stacking Absorbers

For the EFIG material, there is an initial 2-4 dB reduction in *Q* resulting from adding the first absorber. Adding the second absorber yields roughly another 2 dB in *Q* reduction, but the third, fourth, and fifth absorbers add very little change at the lower frequencies and no further reduction above 8 GHz. The WXA material provides approximately 3 dB of *Q* reduction at the lower frequencies, but that begins to decline at around 7.5 GHz. At any given frequency, there is only approximately 1 dB or less of additional *Q* reduction by using more than 1 piece of WXA. KPIG follows a similar trend. There is initially around 5 dB of *Q* reduction from the first absorber. For frequencies below 8 GHz, additional absorbers yield approximately 2 dB more *Q* reduction, but there is practically no difference between 2, 3, 4, or 5 absorbers. Above 8 GHz, there is no marginal benefit to using more than 1 piece of KPIG. The UD material is the first material that

continually reduces *Q* with each additional sheet, but the marginal increase in *Q* gets smaller and smaller with each additional absorber. Each material experiences a reduction in effectiveness in reducing *Q* above 8 GHz. Tables 4-1 through 4-4 highlight some key features of the plots for each material.

Table 4-1: EFIG Stacking Results

	1 Sheet	**2 Sheets**	**3 Sheets**	**4 Sheets**	**5 Sheets**
Optimal Center Frequency	7.5 GHz	7.5 GHz	7.5 GHz	7 GHz	7 GHz
Maximum *Q* Reduction	3.79 dB	5.97 dB	6.93 dB	7.02 dB	7.12 dB
Average Marginal *Q* Reduction	3.08 dB	2.04 dB	0.64 dB	-0.02 dB	0.15 dB

Table 4-2: WXA Stacking Results

	1 Sheet	**2 Sheets**	**3 Sheets**	**4 Sheets**	**5 Sheets**
Optimal Center Frequency	7.5 GHz	6 GHz	5.5 GHz	7 GHz	7 GHz
Maximum *Q* Reduction	4.16 dB	3.81 dB	3.92 dB	3.90 dB	4.71 dB
Average Marginal *Q* Reduction	3.00 dB	-0.30 dB	-0.07 dB	0.30 dB	0.75 dB

Table 4-3: KPIG Stacking Results

	1 Sheet	**2 Sheets**	**3 Sheets**	**4 Sheets**	**5 Sheets**
Optimal Center Frequency	7.5 GHz	7.0 GHz	7.0 GHz	7.5 GHz	7.5 GHz
Maximum *Q* Reduction	6.33 dB	7.72 dB	7.32 dB	7.45 dB	7.80 dB
Average Marginal *Q* Reduction	5.39 dB	0.83 dB	-0.04 dB	0.23 dB	0.23 dB

Table 4-4: UD Stacking Results

	1 Sheet	2 Sheets	3 Sheets	4 Sheets	5 Sheets
Optimal Center Frequency	7 GHz	7 GHz	7 GHz	7 GHz	7 GHz
Maximum *Q* Reduction	7.13 dB	7.77 dB	8.42 dB	8.96 dB	9.47 dB
Average Marginal *Q* Reduction	5.90 dB	0.65 dB	0.64 dB	0.52 dB	0.47 dB

All of the materials suffered from severely diminishing returns in regards to the amount of reduction of *Q* compared to the amount of absorbers used.

Figure 4-12 shows the results of spreading the sheets of absorbers to different surfaces of the cavity.

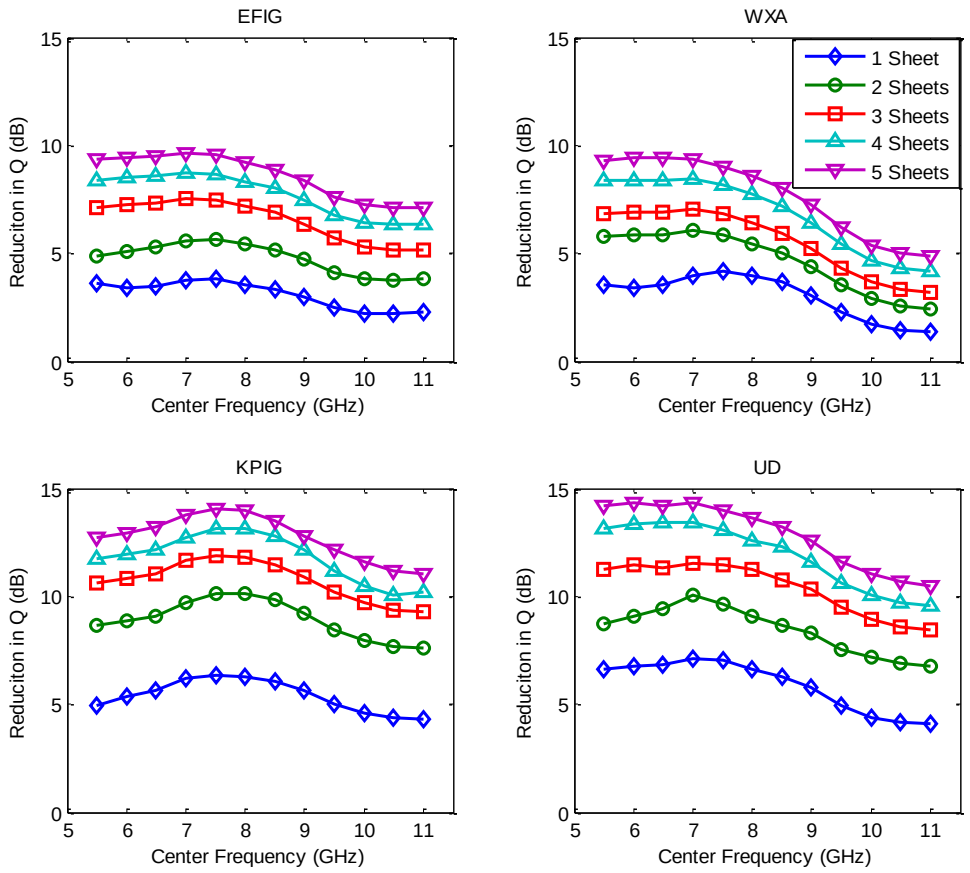

Figure 4-12: Results from Spreading Absorbers

Spreading the absorbers to different walls allows each piece of absorber to further reduce the *Q* of the cavity whereas the plots when stacking were often overlapping one another. All materials except for KPIG follow the same trend with a gradual decrease in *Q* reduction at the lower frequencies, a steeper decrease in *Q* reduction in the middle frequency ranges, and returning to a gradual decrease in the higher frequency ranges. The KPIG material gradually increases in the lower to middle frequency ranges, then begins to decrease in the middle to high frequency ranges. Tables 4-5 through 4-8 highlight some key characteristics of the plots for each material.

Table 4-5: EFIG Spreading Results

	1 Sheet	2 Sheets	3 Sheets	4 Sheets	5 Sheets
Optimal Center Frequency	7.5 GHz	7.5 GHz	7 GHz	7 GHz	7 GHz
Maximum *Q* Reduction	3.79 dB	5.62 dB	7.52 dB	8.72 dB	9.65 dB
Average Marginal *Q* Reduction	3.08 dB	1.69 dB	1.76 dB	1.18 dB	0.87 dB

Table 4-6: WXA Spreading Results

	1 Sheet	2 Sheets	3 Sheets	4 Sheets	5 Sheets
Optimal Center Frequency	7.5 GHz	7 GHz	7 GHz	7 GHz	6 GHz
Maximum *Q* Reduction	4.16 dB	6.03 dB	7.02 dB	8.43 dB	9.42 dB
Average Marginal *Q* Reduction	3.00 dB	1.64 dB	0.91 dB	1.27 dB	0.84 dB

Table 4-7: KPIG Spreading Results

	1 Sheet	2 Sheets	3 Sheets	4 Sheets	5 Sheets
Optimal Center Frequency	7.5 GHz	7.5 GHz	7.5 GHz	7.5 GHz	7.5 GHz
Maximum *Q* Reduction	6.33 dB	10.13 dB	11.91 dB	13.14 dB	14.06 dB
Average Marginal *Q* Reduction	5.39 dB	3.57 dB	1.78 dB	1.08 dB	0.93 dB

Table 1: UD Spreading Results

	1 Sheet	2 Sheets	3 Sheets	4 Sheets	5 Sheets
Optimal Center Frequency	7 GHz	7 GHz	7 GHz	6.5 GHz	6 GHz
Maximum *Q* Reduction	7.13 dB	10.03 dB	11.57 dB	13.46 dB	14.36 dB
Average Marginal *Q* Reduction	5.90 dB	2.54 dB	1.96 dB	1.50 dB	0.96 dB

This trend of spreading absorbers resulting in lower *Q* than stacking was attributed to the absorbers covering more of the reflective surfaces of the cavity which resulted in fewer attenuation free reflective paths for the waves to travel. A simple mathematical model was developed in order to explain why spreading absorbers had a larger impact on reducing *Q* than stacking them.

In [14], Hill describes the field at any point in the working volume as a sum of plane waves. Any one of these waves has an arbitrary direction and pseudo arbitrary magnitude. This wave can reflect around the cavity until it has fully decayed. If an arbitrary starting point is chosen, a wave could be traveling in any direction and that particular direction will have some specific reflective path. For any point in the working volume, the total paths can be defined by the following equation:

$$P_{total} = \sum_{n=0}^{\infty} A_n P_n \tag{7}$$

where

P_{total} is the set of all possible paths.

P_n is the subset of paths that pass through the absorber n times.

A_n is the combined amplitudes for P_n.

The absorbers have some attenuation constant, α, and the resulting amplitude of a subset of waves, R , with any value of n in the cavity can be described as:

$$R_n = (1 - \alpha)^n \tag{8}$$

For a simple example, assume that n is limited to 4, A is equal to 1 for all values of *n*, and α is equal to 0 (no absorbers). The total remaining amplitudes can be described as:

$$\sum_{n=0}^{4} R_n = 1 + 1 + 1 + 1 + 1 = 5 \tag{9}$$

Adding in a single absorber with α = .3, the previous example changes to:

$$\sum_{n=0}^{4} R_n = 1 + 0.7 + 0.49 + 0.34 + 0.21 = 2.773 \tag{10}$$

By stacking a second absorber, the net α becomes .51 (a wave incident on the absorbers would attenuate 30% then 30% again for the second absorber), but no more paths pass through the absorber than they did before and the remaining amplitudes become:

$$\sum_{n=0}^{4} R_n = 1 + 0.49 + 0.240 + 0.118 + 0.058 = 1.905 \tag{11}$$

The initial absorber resulted in 44.5% attenuation, but the second absorber only resulted in 61.9% attenuation. Alternatively, if the second absorber had been placed in a new location, then *n* could have been increased. For simplicity, assume that by placing the absorber on a second surface, *n* for all paths increased by 2 and α remains at 0.3. The resulting amplitudes would become:

$$\sum_{n=2}^{6} R_n = 0.49 + 0.34 + 0.21 + 0.17 + 0.12 = 1.36 \tag{12}$$

These examples were greatly oversimplified, but they provided a basis for further experimentation in the optimization of absorber usage.

4.4 Absorber Cross Section vs Absorber Volume

The results from the Surface Area vs Volume experiment led to the notion that the thickness of the absorber has severe diminishing returns on *Q* reduction. In order to test this notion, an experiment was performed in which 5 sheets of material were stacked and the centers were removed one layer at a time from bottom to top. An illustration of the absorber configurations can be seen in Figure 4-13.

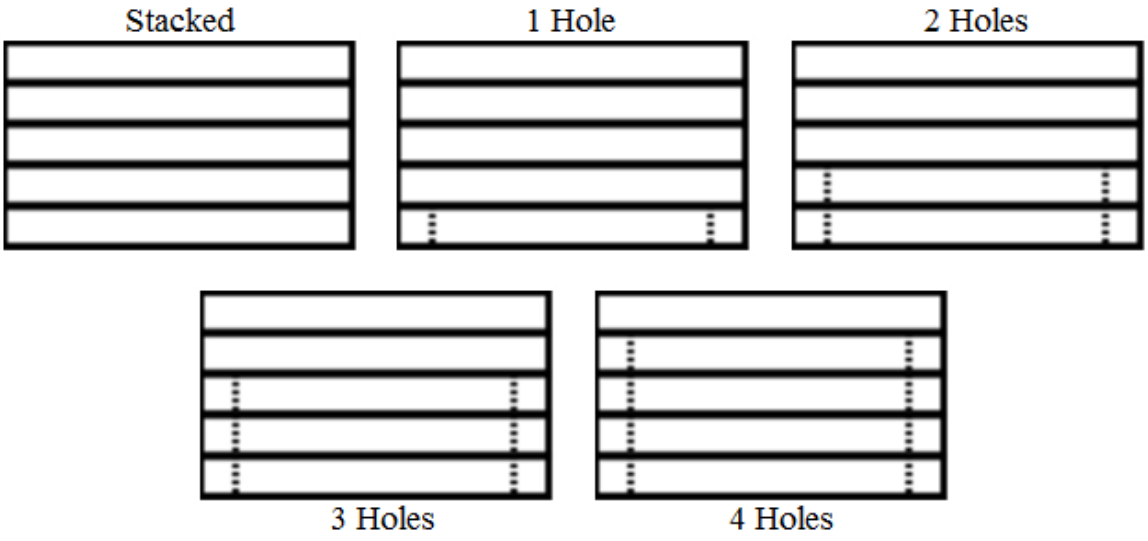

Figure 4-13: Cross Section vs Volume Loading Setups

By removing the material, the occupied volume remains the same while the amount of material used is greatly reduced. To put this in perspective of the previous experiment explanation, n should remain the same while α is being lowered. The resulting *Q* values can be seen in Figure 4-14.

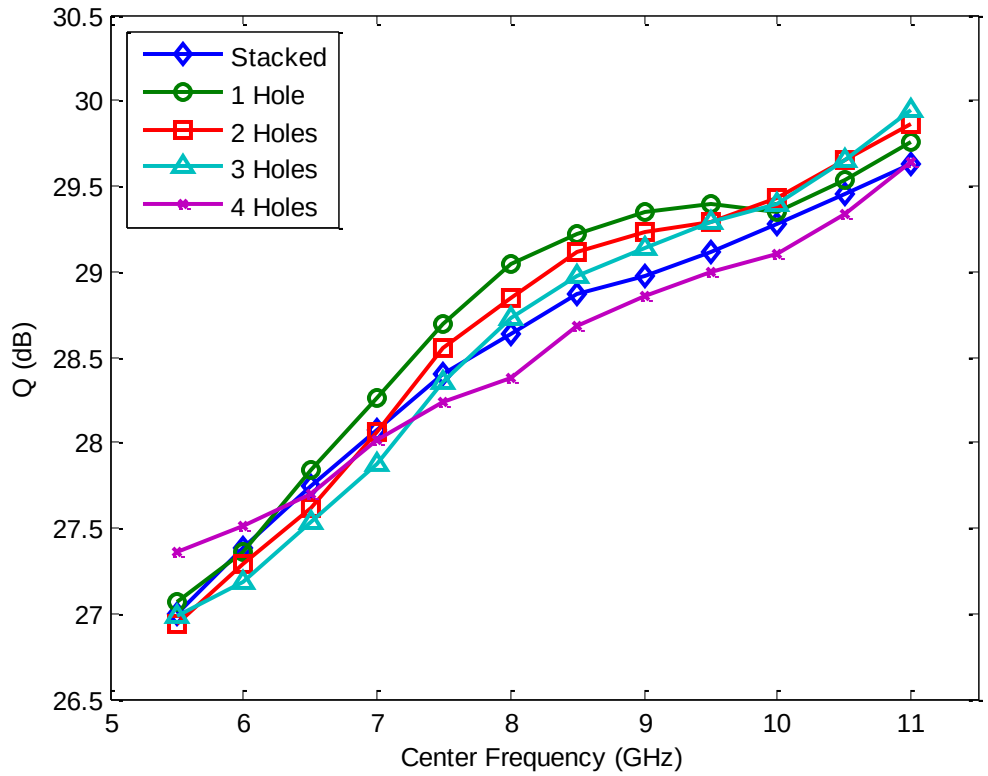

Figure 4-14: Cross Section vs Volume Results

This figure shows that removing material from the bottom layers has a negligible effect on *Q*. This could be because the paths passing through the absorbers have already been heavily attenuated and affecting new paths would be more beneficial. It is also possible that the skin depth of the absorbers is small, and having solid absorbers is inefficient. Up until this point, it had been assumed that the majority of attenuation was a result of the top side of the absorbers since it provided the most surface area and cross section. The following tests explored what would happen if the fifth layer was bored out like the bottom four. Two additional tests were performed with the five rings stacked and spread. The results of these tests can be seen in comparison with the previous test in Figure 4-15.

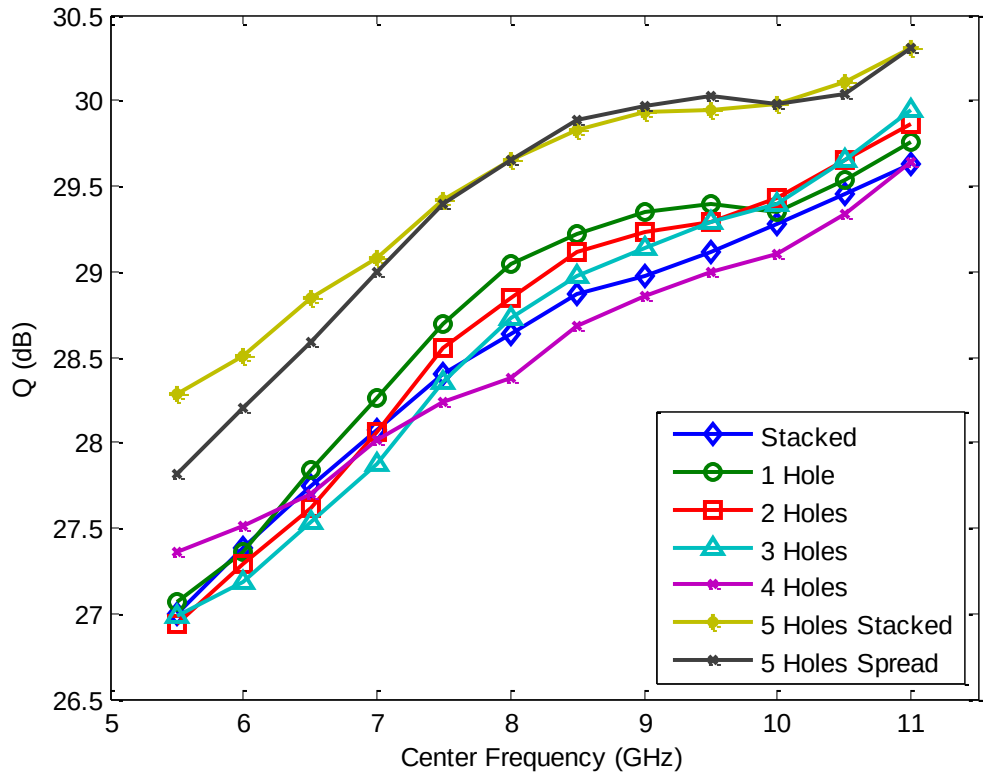

Figure 4-15: Cross Section vs Volume Final Results

The *Q* of the cavity is approximately 1 dB higher until around 8 GHz. This is the expected behavior because the exposed surface area has been reduced. The results from stacking the 5 rings are also consistent with the reflective path theory because removing the final center creates more attenuation free paths. The results from spreading the five rings, however, do not follow the expected trend. In all previous experiments, increasing exposed surface area while maintaining the same volume resulted in a reduction in *Q*. This discovery gave rise to the question of how the waves interacted with the space in between the absorbers while simultaneously derailing the reflective path theory proposed in Section 4-3. In an attempt to explain this new phenomenon, an experiment was designed to investigate how absorber spacing played a role in *Q* reduction.

4.5 Absorber Spacing

In order to attempt to reduce the complexity of these experiments, the amount of material used in the following experiments was reduced to 100 cm^2. Rather than removing the inner sections of the material, the material was cut into smaller pieces and placed with specific spacing in between the pieces. Due to it having the largest impact on Q, the UD material was used. For the first spacing experiment, the 10 cm × 10 cm sheet was cut into two 5cm × 10 cm sheets. The spacing between the pieces was incremented from 0 to 5 cm in 1 cm steps. Figure 4-16 shows an illustration of the test setup.

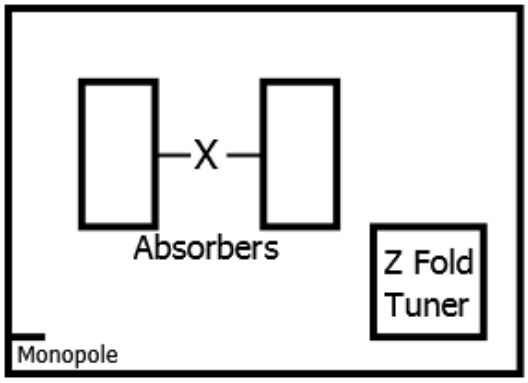

Figure 4-16: First Spacing Test Setup

The *Q* value was measured for the same 12 frequency bands as the previous experiments. The resulting *Q* values can be seen in Figure 4-17.

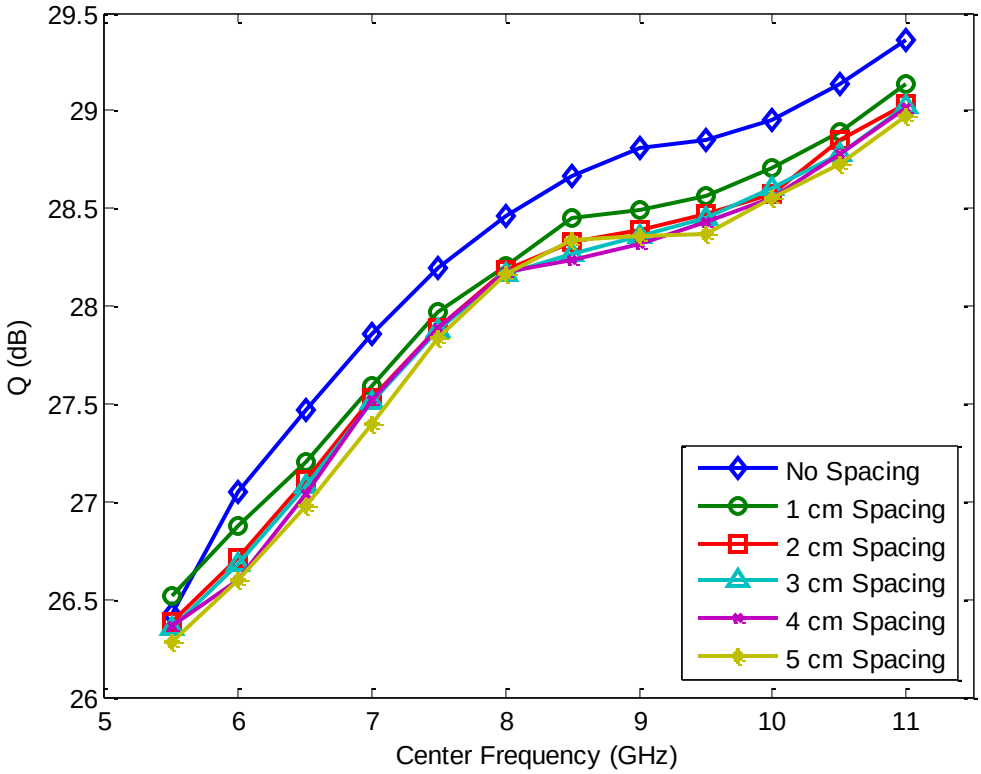

Figure 4-17: 2 Piece Spacing Results

Other than the 5.5 GHz band, there was a small decrease in *Q* from spacing the absorbers 1 cm apart. There was a marginal decrease in *Q* by spacing 2 cm apart, but there was little to no benefit from spacing beyond 2 cm. The next step of this spacing experiment was to cut the two 5 cm x 10 cm pieces into four 5 cm x 5 cm pieces. The spacing in 1 direction was fixed at 1 cm, while the spacing in the other direction was incremented from 1 to 4 cm in 1 cm steps. Figure 4-18 shows an illustration of this loading procedure.

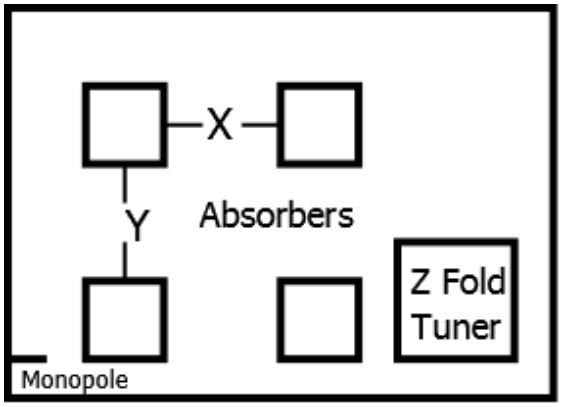

Figure 4-18: 4 Piece Spacing Setup

The results of the first 4 Piece Spacing test can be seen in Figure 4-19.

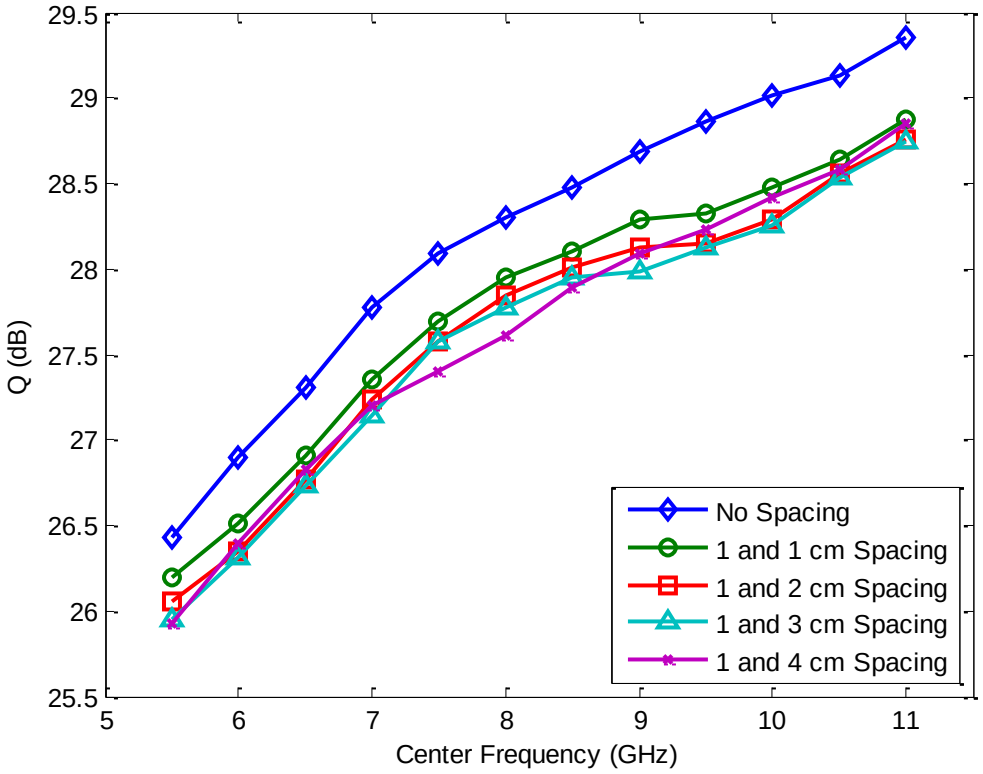

Figure 4-19: 4 Piece Spacing First Experiment Results

As with the 2 Piece Spacing experiment, there is a decrease in *Q* from initially spacing the absorbers, but there is very little to no benefit from spacing beyond 2 cm. This test was primarily performed as a basis of comparison for the next test. In the following test, the spacing in both directions was incremented from 1 to 4 cm in 1 cm steps. Figure 4-20 shows the results from the second 4 piece spacing test.

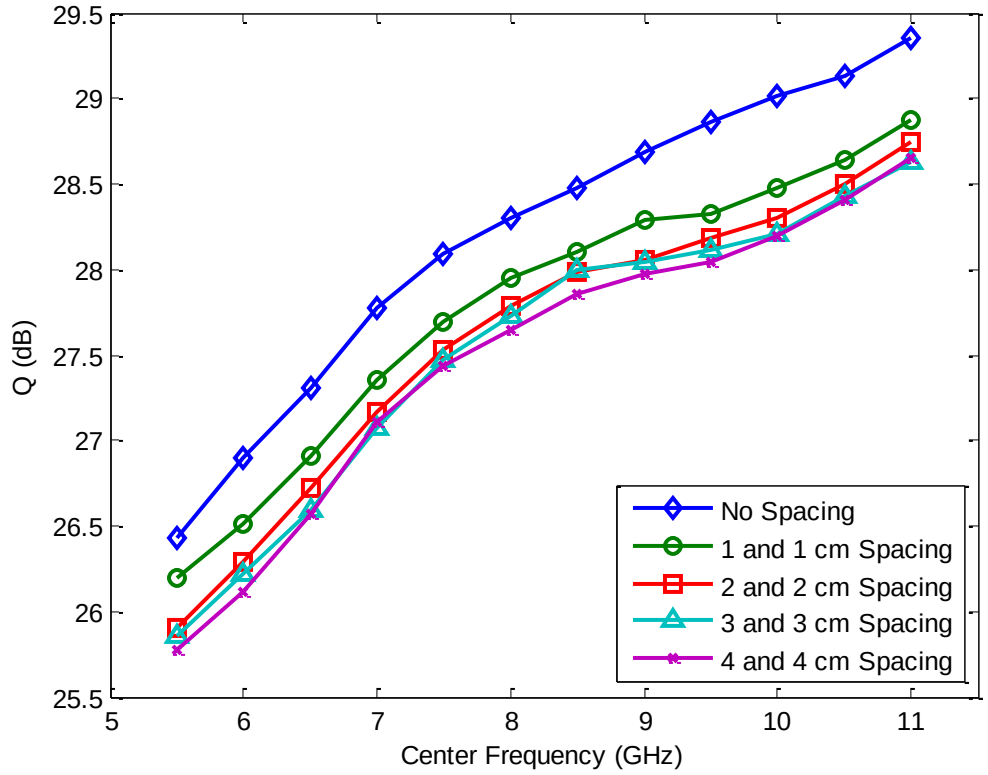

Figure 4-20: 4 Piece Spacing Second Experiment Results

As with the other spacing experiments, there is a slight reduction in *Q* by spacing from 1 cm to 2 cm. For the most part, 3 cm is marginally better, but 4 cm is practically the same as 3 cm. It was decided to take this experiment one step further. The four 5 cm × 5 cm pieces were cut into sixteen 2.5 cm × 2.5 cm pieces and spaced 2 cm apart. Figure 4-21 shows a comparison of the

resulting *Q* values from a single 10 × 10 piece, the four 5 × 5 pieces spaced 2 cm apart, and the sixteen 2.5 × 2.5 pieces spaced 2 cm apart.

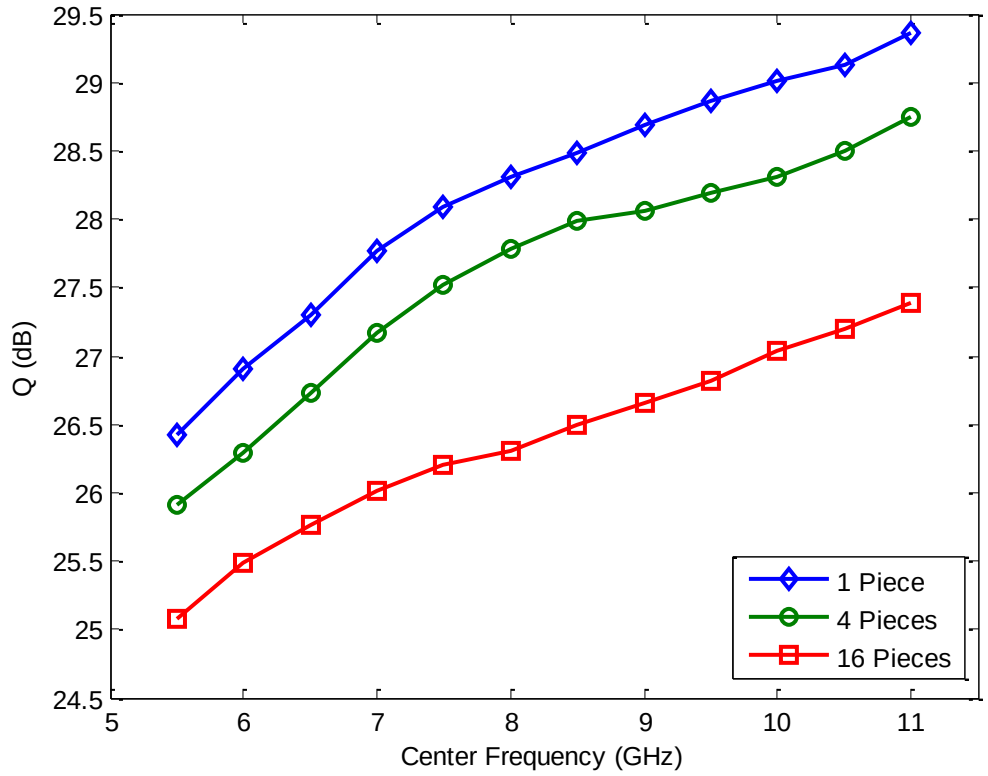

Figure 4-21: Final Spacing Comparison

This plot demonstrates that cutting the absorbers into smaller pieces and spreading them out results in a lower *Q* value. There is roughly a 0.7 dB reduction in *Q* going from 1 large piece to 4 smaller pieces and another 1 dB reduction in *Q* going from 4 pieces to 16 smaller pieces. It is worth noting that this could be due to the increased exposed surface area from cutting and separating the pieces. While there was not any additional reflective surface being covered, there was more exposed surface area of the material. One thing that was common with all of the spacing tests was that the absorbers were spaced with each piece being aligned into an array. The results were somewhat indicative that the spaced absorbers were performing almost as if there

was no spacing in between them. Unfortunately it is not feasible to manufacture the absorbers into such small pieces and install them into a cavity piece by piece. To emulate a solid single piece of absorber with sections removed, the 16 pieces were placed into a checkerboard pattern, which can be seen in Figure 4-22.

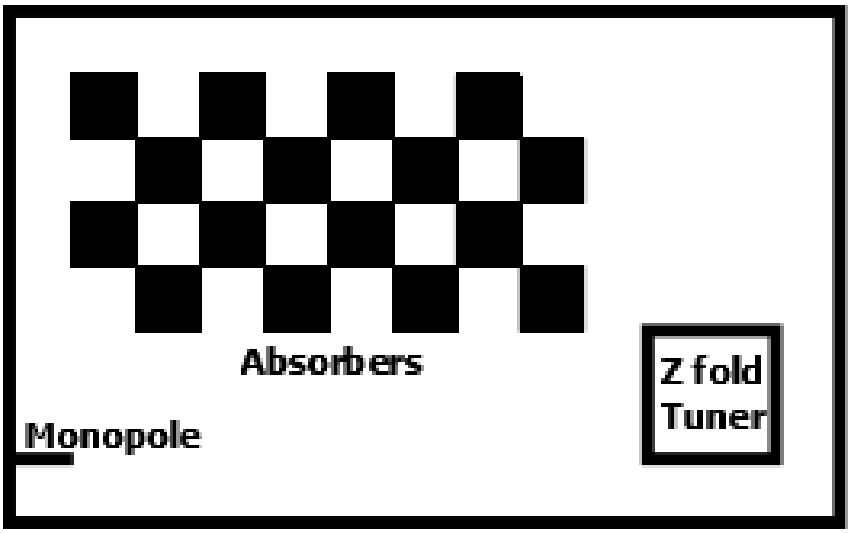

Figure 4-22: Checkerboard Absorber Illustration

Figure 4-23 shows a comparison of the *Q* values that were measured for the 2 cm spacing from the previous experiment and the new checkerboard spacing pattern.

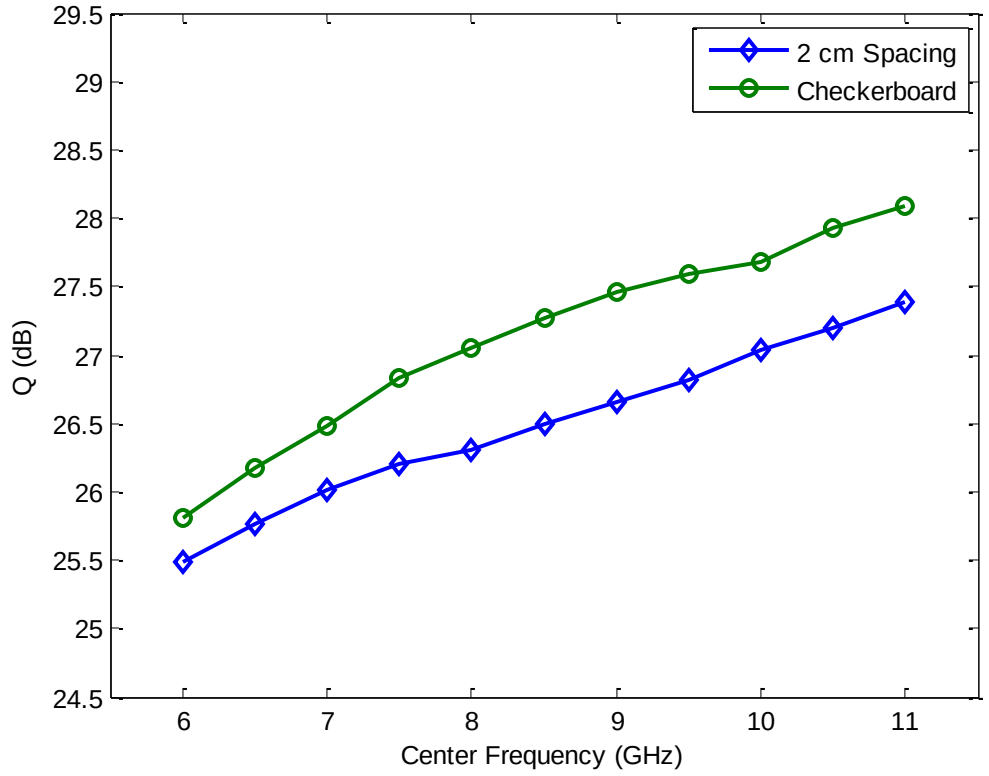

Figure 4-23: Array vs Checkerboard Spacing Results

There was approximately a 0.5 dB decrease in *Q* reduction from placing the absorbers into the checkerboard pattern. This indicates that spacing in all directions including diagonally yields the best performance. None of the spacing requirements resulted in more reflective paths being removed. This theory has been disproven in every experiment since its inception. The theory about exposed surface area has been consistent with the spacing results, but another factor to consider is that the absorbers were spanning a wider area of the cavity which would allow more modes to be affected. In order to remove the second variable, a new experiment was developed to increase the surface area without spreading the absorbers or protruding closer to the working volume.

4.6 Ridged Absorber Experiments

In order to increase the surface area of an absorber without increasing the height or changing the cross section, a design was developed in which a square sheet of absorber was taken and ridges were cut halfway down the material. Figure 4-24 shows an illustration comparing the smooth absorber with the ridged absorber.

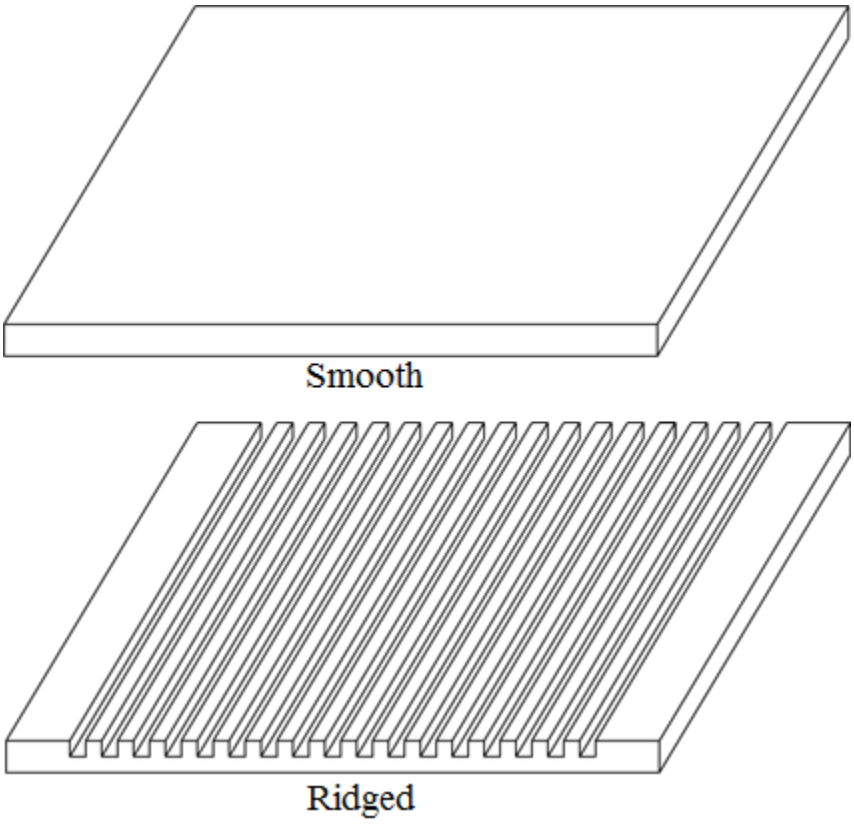

Figure 4-24: Smooth and Ridged Absorber Examples

Figure 4-25 provides a comparison for the *Q* calculations between the smooth and ridged absorber.

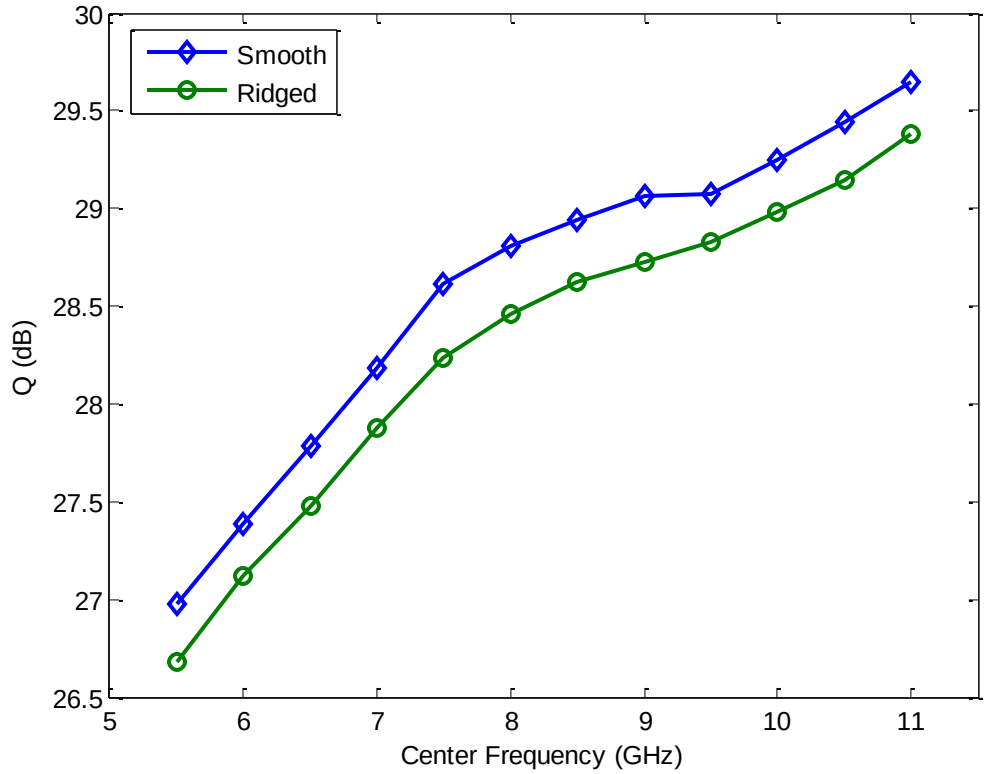

Figure 4-25: Ridged Absorber First Experiment Results

There was a .3 dB difference in *Q* across all frequency bands. While 0.3 dB of a reduction in *Q* is rather small, it is interesting because the ridged piece contains less material due to the ridges having been cut out. To take this a step further, another piece of absorber was modified to have ridges cut in both directions to expose even more surface area. Figure 4-26 shows an illustration of the cross-ridged pattern.

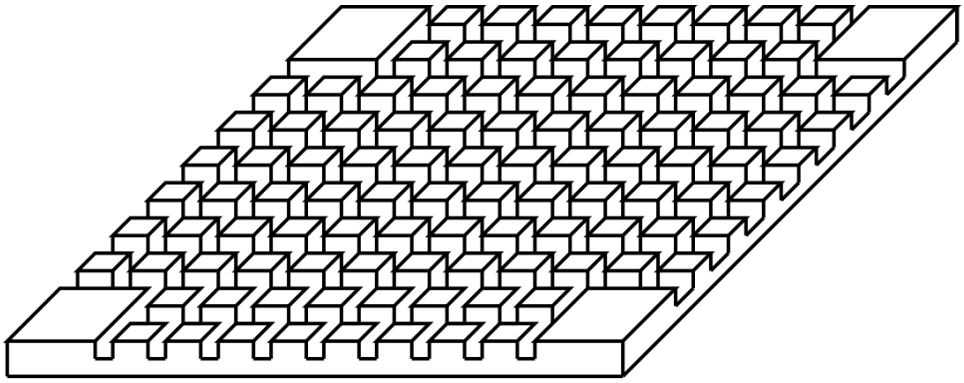

Figure 4-26: Cross Ridged Absorber Example

The results comparing the cross ridged absorber with the ridged and smooth absorbers can be seen in Figure 4-27.

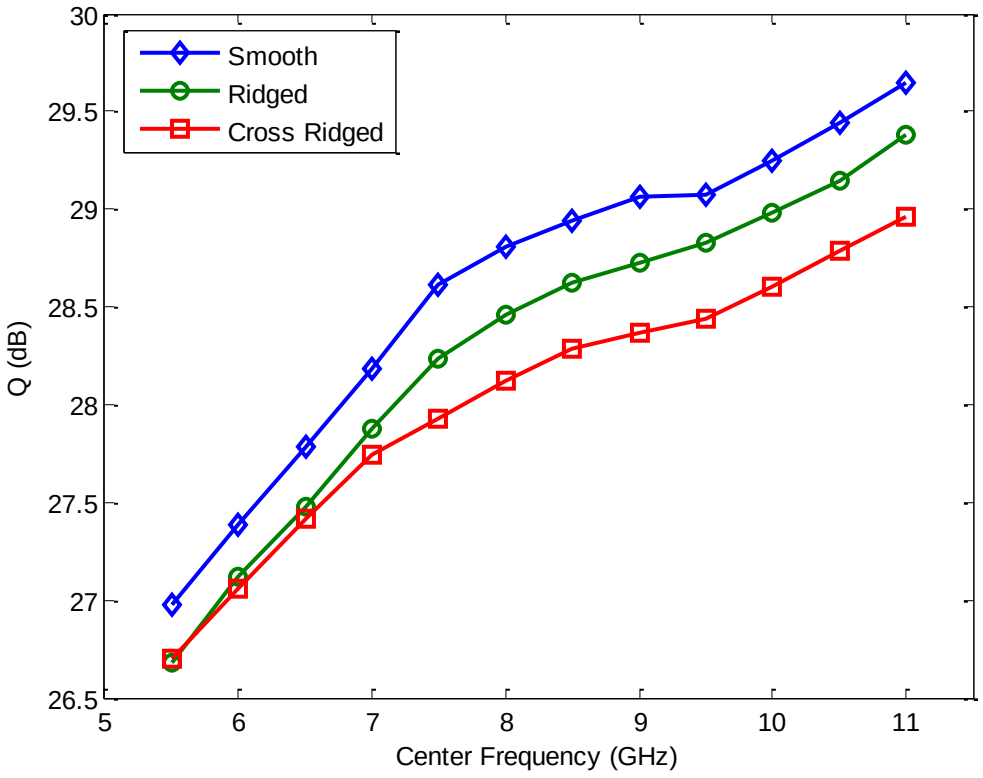

Figure 4-27: Second Ridged Absorber Experiment Results

At the lower frequencies there was very little difference between the ridged absorber and the cross-ridged absorber, but at frequencies above 7 GHz, there was a 0.4 dB reduction in *Q* compared to the ridged absorber and a 0.7 dB reduction in *Q* compared to the smooth absorber. The better performance at higher frequencies could have been due to the ridges being very small. As the frequency increased, the wavelength decreased which might have allowed the small ridges to have more impact. Further testing would be required with different sized ridges to compare performance against frequency. In order to verify that these results were not just measurement error, the test was repeated, but the absorbers were placed in a corner rotated by 45 degrees rather than the middle of the floor aligned with the walls. The results of this verification test can be seen in Figure 4-28.

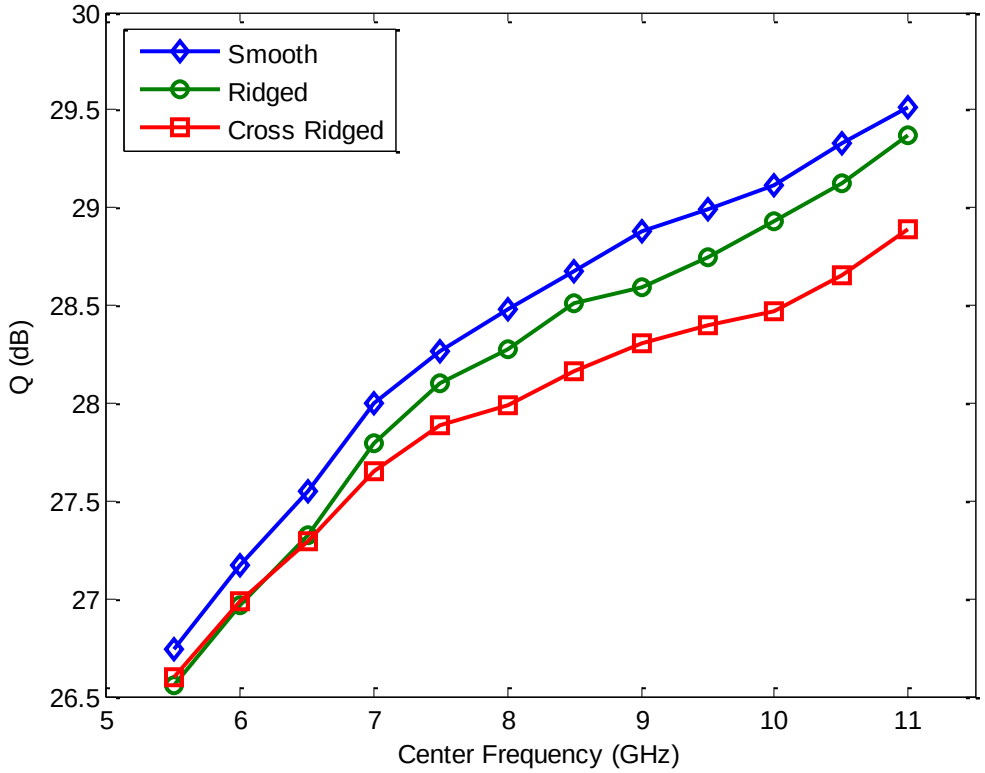

Figure 4-28: Results from Ridge Experiment Verification

The values were approximately 0.2 dB lower overall, but the trends were the same. Absorbers with ridges had a *Q* value of roughly 0.3 dB less than the smooth absorber for all frequency bands. The cross-ridged absorber's performance relative to the ridged absorber's performance increased with frequency starting above 7 GHz, and there was about 0.4 dB of separation between them above 7 GHz. Although the resulting reduction in *Q* from adding the ridges to the absorber was small, this was still an important discovery because higher attenuation could be achieved using less material which saves cost and weight.

4.7 Bandwidth Requirements

An underlying concern in regards to these "time domain" *Q* measurements is their wide bandwidth requirements. The true *Q* of the cavity is a function of frequency[11]. By calculating a single *Q* over a large bandwidth, concerns arise about the validity or physical meaning of the *Q* calculated. The bandwidth requirement was established in Green's work [9] but was based on the assumption that the pulse width was required to be shorter than the wall scattering time. The pulse was required to be shorter than the wall scattering time to prevent energy that was will being injected into the cavity from skewing the measurement of the energy decay. The validity of this claim came into question. This claim was compared to measuring the effect of gravity. In the same regards that it would not matter how long it took an object to reach its highest point, the rate that the object falls will be the same. Similarly, it should not matter if it takes longer to inject energy into the cavity. The rate of decay will still be the same after the energy is injected. An experiment was created to test this theory. The *Q* values were measured for an empty cavity and a loaded cavity over the same 12 frequency bands used for the previous experiments. The bandwidths for each measurement were reduced in half for each experiment ranging from 5 GHz to 312.5 MHz. Figure 4-29 shows the resulting *Q* values for both experiments.

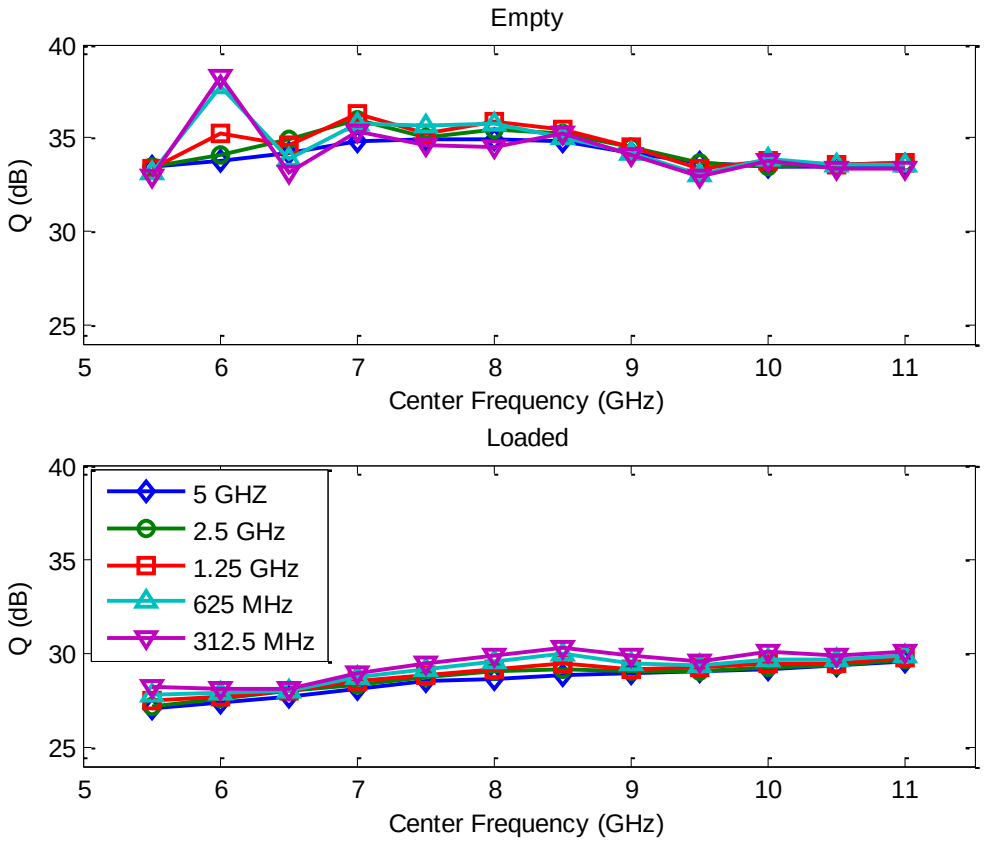

Figure 4-29: Bandwidth Requirement Results

There is a very strong agreement between the *Q* trends regardless of the bandwidth chosen, with the exception of the 625 MHz and 312.5 MHz results for the empty cavity. While there may be minor discrepancies between the results from one bandwidth to the next, it is important to remember that these time domain *Q* values are actually combining all of the *Q* values over the entire bandwidth into a single number so the actual *Q* numbers are much less important than the trends in *Q* and the change in *Q* from one loading setup to another. In terms of being able to quantify the change in *Q* from one loading to the next, using bandwidth wide enough to reduce the pulse time below the wall scattering time is not a requirement.

Section 4.8 - Emissions Results

This research has discovered multiple ways to effectively reduce the *Q* of a cavity through loading with absorbers. Unfortunately, there has not been any proof that reducing the *Q* of a cavity will directly reduce the emissions from that cavity. The initial emissions measurements were designed to measure the maximum emissions from the cavity. The monopole inside the small cavity was connected to a signal generator. The signal generator output power level was set to +18 dBm and the center frequency of the ramp sweep mode was set the 5.5 GHz. The receiving antenna was outside the small cavity in the SMART 80 chamber and connected to a spectrum analyzer that was configured to sweep over the same bandwidth as the signal generator in 1 MHz steps and the resolution bandwidth was initially set to 300 kHz. The sweeps were run for 6 hours each (over 46 times the fundamental period of the tuners) in order to collect preliminary test results. The purpose of this experiment was to verify that by placing the spectrum analyzer on a max hold setting, the two tuners would reach every possible combination of positions and the maximum emissions would be captured. The results of the initial maximum emissions experiment can be seen in Figure 4-30.

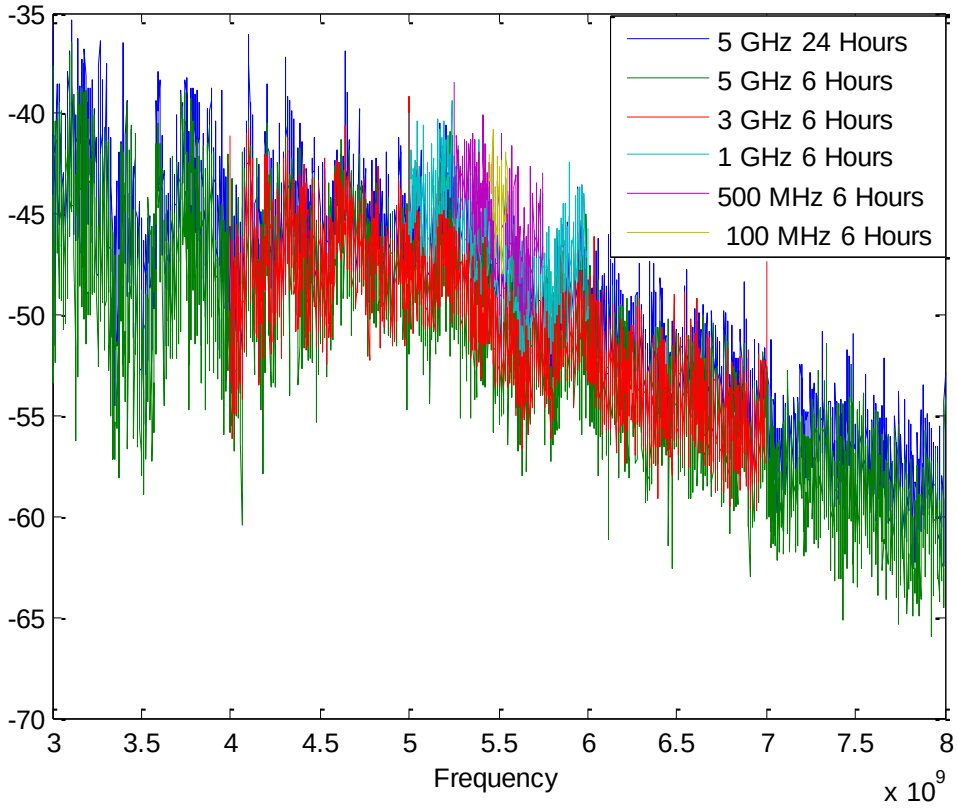

Figure 4-30: Preliminary Maximum Emissions Results

The maximum power received varied greatly from one experiment to the next. Many of these fluctuations are greater than 5 dB. The primary concern was that this test was unreliable and had little to no repeatability. A secondary test was performed using the signal generator in CW mode (single frequency) and only a 100 MHz bandwidth for the spectrum analyzer. The experiment was performed 12 times for 10 minute intervals (still greater than the fundamental period for the tuners). The results of the secondary emissions test can be seen in Figure 4-31.

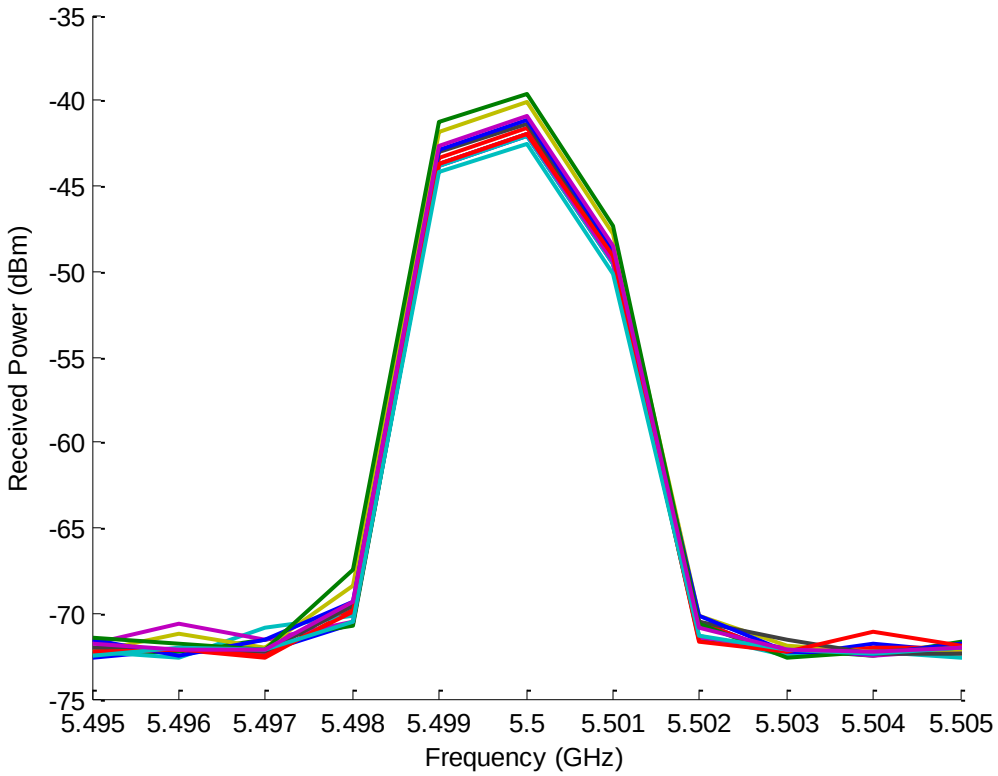

Figure 4-31: Secondary Maximum Emissions Results

Unfortunately even with only a single frequency being measured, there was up to almost 4 dB of variation between the maximum powers received. It was at this time that a realization was made that measuring a peak value in a reverberation chamber was not going to be a feasible approach. The primary reason for using a reverberation chamber is to rely on a statistical approach using a large number of samples and averaging. As a result, maximum emissions were forgone, and the approach to measure the average power received was developed.

Using the process outlined Section 3.5, the cavity was placed under 11 different loading conditions. The *Q* and average power radiated from the cavity were measured for each loading setup for three frequency bands. The change in *Q* was calculated and plotted with the corresponding change in emissions. Figure 4-32 shows the resulting plots.

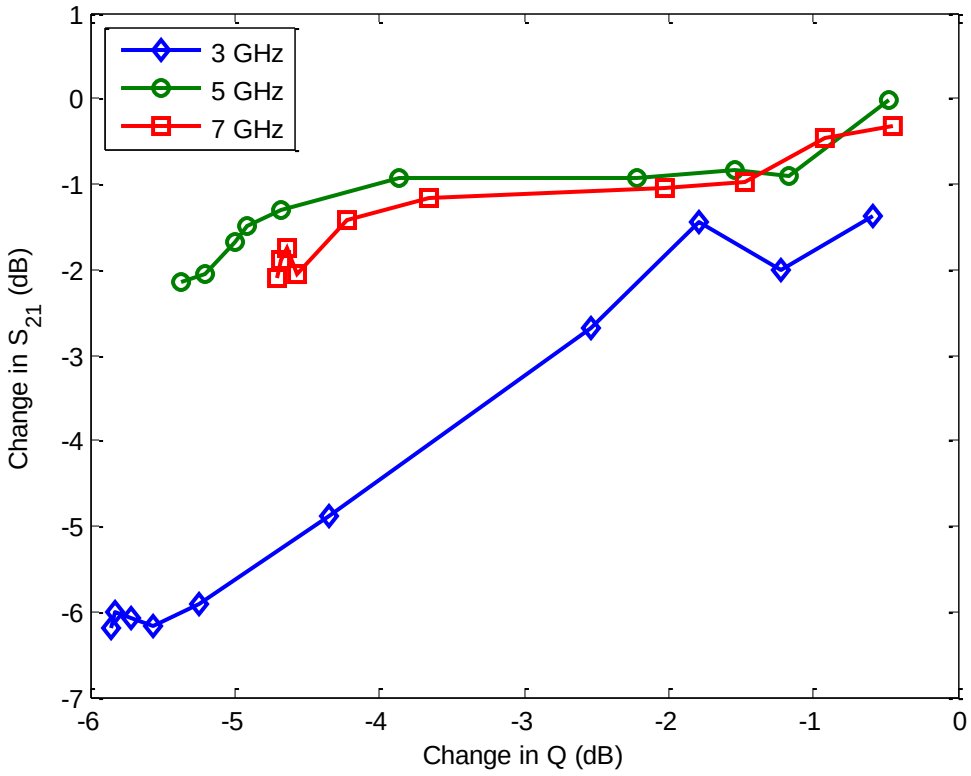

Figure 4-32: Emissions vs *Q* Initial Results

The results of the 3 GHz measurements were mostly as expected. There is a mostly linear trend between the reduction in *Q* and the reduction in the average S_{21} data. The 5 GHz and 7 GHz plots, however, did not behave as expected. There are changes in *Q* of almost 3 dB with only about 0.5 dB reduction in emissions in some areas, but in other parts of the plots, a 0.5 dB reduction in *Q* yields a 0.5 reduction in emissions. These initial emissions values were only calculating the average S_{21} values at the center frequency. The average S_{21} values were recalculated using the average S_{21} values for the entire frequency band and the corresponding plots can be seen in Figure 4-33.

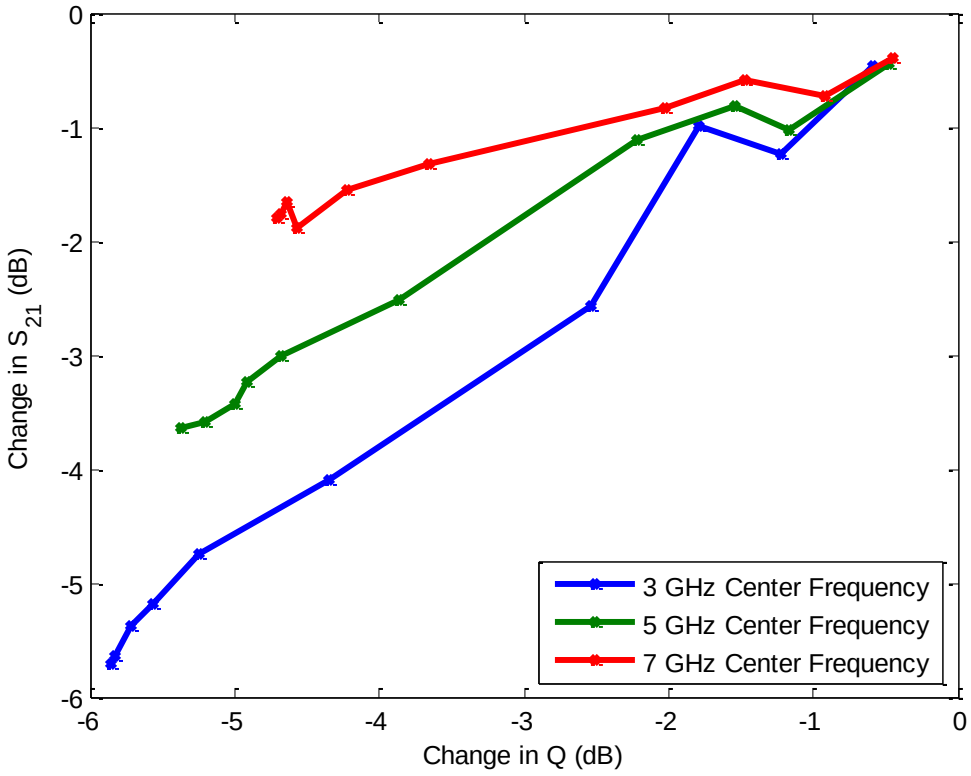

Figure 4-33: Emissions vs *Q* Final Results

These new plots follow much more linear trends. Each curve has an uncharacteristic increase in S_{21} for the third loading setup. For this to appear in all three frequency bands for the same loading setup is an unlikely coincidence. At this time, correlation coefficients were calculated between the change in *Q* values and the corresponding change in S_{21} values for each frequency band. A correlation coefficient, R, is a statistical calculation between two variables. R can range from -1 to 1. A larger magnitude indicates a stronger the linear relationship between the two variables. A correlation coefficient of 1 indicates that the relationship is completely, positively linear. In addition to calculating the correlation coefficients, the line of best fit for each curve was calculated. The lines of best fit were used to calculate the slopes relating change in S_{21} to change in Q. Table 4-9 summarizes the linear relationships between reduction in *Q* and reduction in S_{21}.

Center Frequency	Correlation Coefficient, R	Slope ($\Delta S_{21}/\Delta Q$)
3 GHz	0.993	0.982
5 GHz	0.990	0.671
7 GHz	0.980	0.321

Table 4-9: Correlation Results Summary

There is almost a completely linear relationship between reduction in *Q* and reduction in emissions at all three frequency bands. Reduction in *Q* and reduction in emissions have an undeniable correlation. The amount of reduction in S_{21} per reduction in *Q*, however, is very much frequency dependent. This means that with a relatively high level of certainty, one can say that reducing the *Q* through loading a cavity will reduce the emissions from that cavity, but there is still not an easy way to determine how much reduction in *Q* is required to reduce emissions by a specific amount. One possible explanation is the radiation efficiency of the aperture at a given frequency, but it is unlikely that the change in the ratio between *Q* reduction and emissions reduction is due to the aperture dimensions since the aperture had a slot resonance at all three center frequencies. Based on the three data points that are available, the relationship appears linearly inversely proportional to frequency. No conclusions can be drawn about the slopes without further testing.

CHAPTER V

Conclusions and Future Work

Before this research, there existed very little research in the area of optimization of RF absorber usage in EM emissions reduction. Green performed the preliminary work by establishing the VNA based one port time domain approach for measuring the *Q* of a reverberant cavity. This one port technique provided a quantifiable way to measure an effect that the absorbers have on the cavity. Green also experimented with the positional dependence of absorbing materials and found them to be positionally independent provided that the fields inside the cavity were reverberant. This was the extent of Green's investigation into the optimization of absorber usage. This research examined the marginal increase in performance from stacking additional absorbers as well as spreading the absorbers to different surfaces within the cavity. Since spreading the absorbers was consistently causing a larger reduction in *Q* than stacking, two theories arose as possible explanations.

Existing work about the use of absorbers in reverberation chambers attributed absorber surface area as the primary factor contributing to the absorbers performance. This research presented an alternative theory based on the presumed reflective paths derived from Hill's plane wave integral explanation of the fields inside the working volume of a reverberation chamber. This theory was tested by removing the center material from the lower absorbers one layer at a time. The initial

.

results indicated that there was little difference between 5 solid absorbers and a single solid absorber placed on top of 4 hollow ones, which was indicative that the waves were not penetrating deep into the absorbers. This could be a result of the material properties, and additional experiments with different materials could be formed. When the center of the top layer was removed, however, there was only a slight increase in Q, and spreading the 5 rings was almost equivalent to stacking them. This was the only experiment where exposing more surface area did not reduce the *Q* of the cavity. It is possible that this lack of increased performance from spreading the rings was a result of the dielectric properties of the material. Additional work can be completed performing similar experiments with a large variety of materials. By sampling a large variety of materials, it would be possible to see how *Q* reduction correlates with material properties and absorber placement. The next experiment looked at splitting absorbers into smaller pieces and slowly separating them. The results of the spacing tests consistently indicated that spacing absorber pieces at least 2 cm apart results in a lower *Q* than the larger absorbers. *Q* continued to decrease as the absorbers were cut into smaller pieces and separated, but further work is needed with additional materials to verify that this is not material dependent. At this point the reflective path theory was now rejected as well as Green's positional independence. Future work could investigate the positional dependence of additional loading since Green's work only looked at positional dependence for a single absorber. Another method of *Q* reduction was examined in this research during the ridged absorber testing. This experiment showed that the same or lower *Q* values could be obtained with less material. Further investigation could involve materials with larger ridges or perhaps different ridge shapes rather than just straight notches used in this work. Green's work and this research operated under the assumption that the pulse width must be shorter to the wall scattering time, but this has been shown to be a poor assumption. The next step should be to repeat some of the experiments from this work in small with smaller frequency steps to see if any major fluctuations in the *Q* trend are being lost by testing over such a large bandwidth.

In addition to measuring the *Q* of the cavity, a measurement technique for finding the power radiated from the cavity needed to be established. Koepke and Ladbury outlined a procedure utilizing the statistical nature of a reverberation chamber. In their paper, the initial step was to perform a reference measurement using a device with known emissions. In this research, the known device was not actually known, but the empty nested cavity performance was measured as a baseline. Paralleling their example, since nothing was changed in the outer cavity, the outer cavity *Q* remained constant and so the ratio of power transmitted from a device (in this case the small reverberant cavity was the device under test) to the power received by the antenna placed in the larger chamber. The reason that is was not necessary to know the specific emissions level from the empty cavity was simply that the following measurement results were relative comparisons. Since the goal was simply to see if reducing *Q* by X dB would reduce S_{21} by Y dB, it does not matter what the actual initial S_{21} value was. By measuring both the change in *Q* for the smaller cavity and the change in S_{21}, it was possible to determine the correlation coefficient between *Q* reduction and emissions reduction. For all three frequency bands that were tested, the results indicated almost complete correlation between change *Q* and change in emissions although, the amount of emissions reduction per *Q* reduction changed with frequency. This is the most important discovery in this research as it provides a key limitation in that before knowing how much *Q* reduction is required for a target emissions level, the rate of emissions reduction to *Q* reduction has to be known. It is important to note that the reduction in *Q* has to be a result of loading the cavity to reduce emissions. If the *Q* is lowered by adding additional apertures, the emissions will likely rise while the *Q* decreases. At this time it is unknown what factors impact this ratio. It could be the aperture size or aperture shape although the aperture size in this research provided a slot resonance at the center frequencies for each band. More work could be performed using different aperture sizes and frequency ranges to determine if the ratio is linear and inversely proportional as the preliminary findings in this research indicate.

REFERENCES

[1] C. Yang, Q. Zijing, and Z. Xiaonan, "Shielding effectiveness calculation of metallic enclosure with aperture array," in *Antennas, Propagation & EM Theory (ISAPE), 2012 10th International Symposium on*, 2012, pp. 1090-1094.

[2] D. Green, "Analysis and Evaluation of RF Absorbing Material in Suppressing Modes Associated with a Metallic Cavity," Master of Science, Electrical and Computer Engineering, Oklahoma State University, Stillwater, OK, 2014.

[3] V. Rajamani, "Establishing Probability of Failure of a System due to Electromagnetic Interference," PhD, Electrical and Computer Engineering, Stillwater, OK, 2009.

[4] V. Rajamani. (2007, July 5th). *Reverberation Chamber "Statistically Determined Chaos"* [PDF].

[5] R. E. Richardson, "Reverberant Microwave Propagation," 2008.

[6] F. W. a. K. Goldsmith, "Design Philosophy and Material Choice for a Tuner in an Electromagnetic Reverberation Chamber," DSTO Aeronautical and Maritime Research Laboratory, Melbourne Victoria Australia DSTO-TN-0257, February 2000 2000.

[7] D. A. Hill. (1998, Electromagnetic Theory of Reverberation Chambers. *NIST Technical Note 1506*.

[8] V. Rajamani, C. F. Bunting, and J. C. West, "Differences in quality factor estimation in frequency and time domain," in *Electromagnetic Compatibility (APEMC), 2012 Asia-Pacific Symposium on*, 2012, pp. 505-508.

[9] D. L. Green, V. Rajamani, C. F. Bunting, B. Archambeault, and S. Connor, "One-port time domain measurement technique for quality factor estimation of loaded and unloaded cavities," in *Electromagnetic Compatibility (EMC), 2013 IEEE International Symposium on*, 2013, pp. 747-750.

[10] I. RTCA, "Environmental Conditions and Test Procedures for Airborne Equipment," in *Emission of Radio Frequency Energy*, ed. Washington, DC, 2010, pp. 321-343.

[11] G. Koepke and J. Ladbury, "Radiated Power Measurements in Reverberation Chambers," in *ARFTG Conference Digest-Fall, 56th*, 2000, pp. 1-7.

[12] Agilent, ""Time Domain Analysis Using a Network Analyzer"," vol. Application Note 1287-12, ed, May 2012.

[13] G. Tait, M. Slocum, and R. Richardson, "A model to predict reverberant decay time in reflective spaces for wireless applications," in *Wireless and Microwave Technology Conference, 2009. WAMICON '09. IEEE 10th Annual*, 2009, pp. 1-5.

[14] D. A. Hill, "Plane wave integral representation for fields in reverberation chambers," *Electromagnetic Compatibility, IEEE Transactions on*, vol. 40, pp. 209-217, 1998.

VITA

Corey Dylan Vyhlidal

Candidate for the Degree of

Master of Science

Thesis: INVESTIGATING THE CORRELATION BEWTEEN QUALITY FACTOR OF METALLIC CAVITIES AND ELECTROMAGNETIC RADIATION

Major Field: Electrical Engineering

Biographical:

Education:

MASTER of Science in ELECTRICAL ENGINEERING
Oklahoma State University, Stillwater, OK – JULY 2015

BACHELOR of Science in ELECTRICAL ENGINEERING
Oklahoma State University, Stillwater, OK– DECEMBER 2012

Experience:

Oklahoma State University – REFTAS Lab January 2013-Present

Professional Memberships:

INSTITUTE OF ELECTRICAL AND ELECTRONICS ENGINEERS 2012-2013